Assessment of Cold welding between separable contact surfaces due to impact and fretting under vacuum

Issue 3.0 (2025)

A. Merstallinger, M. Sales, E. Semerad, B. D. Dunn *
Austrian Institute of Technology AIT,
A-2444 Seibersdorf/Austria, andreas.merstallinger@arcs.ac.at
* Manufacturing Technology Advisor, Product assurance and Safety Department, ESTEC, Noordwijk/The Netherlands.

Update 2025

A. Merstallinger, R. Holzbauer, N.Bamsey*, A.Tesch*
Aerospace and Advanced Composites GmbH,
A-2700 Wiener Neustadt/Austria,
andreas.merstallinger@aac-research.at, roland.holzbauer@aac-research.at
* Manufacturing Technology Advisor, Product assurance and Safety Department, ESTEC, Noordwijk/The Netherlands.

Abstract:

A common failure mode seen during the testing and operation of spacecraft is termed "cold welding". European laboratories also refer to this as either "adhesion", "sticking" or "stiction". This publication is intended to provide the space community with our most recent understanding of the "cold welding" phenomena as related to spacecraft mechanisms with "separable contact surfaces". It contains some basic theory and describes a test method and required equipment. "Cold welding" between two contacting surfaces occurs under condition of both impact and fretting. These surfaces may be considered as bare metallic, inorganically coated, or organically coated metals and their alloys. Standard procedures for the quantification of the propensity of material surface pairs to "cold weld" to each other are proposed. Of major interest will be the presentation of different materials' contact data which is offered in numerical form and as a Table that summarises those mating contacts that can be either recommended or considered unsuitable for use under vacuum. This data can also be accessed from the world wide web and the relevant site is also detailed.

Keywords: Tribology, cold welding, space, fretting, coatings.

Contents

1 Introduction 4
1.1 Cold welding Failures 4
1.2 Objective to setup test method 5
1.3 Background to Cold welding effect 5
2 Cold welding test method 7
3 State of the art (ESA published data) 9
3.1 Results on Impact 9
3.2 Results on fretting 12
3.3 Influence of coatings on fretting 13
3.4 thin and Thick coatings under fretting anD thermal cycling 15
3.5 Surface morphology after impact and fretting 16
3.6 Influence of contact parameters on fretting / theoretical prediciton of adhesion forces ... 17
4 Data base “Cold Weld Data” 21
4.1 Input for data base 21
4.2 classification of adhesion forces and WEB-data base 21
4.3 WEB-data base: How to access and use 22
5 Conclusion 23
6 Literature 24
6.1 References 24
6.2 Material abbreviations and data to Publications 25
7 Annex A - Description of test devices 26
7.1 Cold welding - Impact and Fretting 26
7.2 Topographic Analysis (Profilometry) 28
8 Annex B –Test method (In-House-Standard) 29
8.1 Scope 30
8.2 General 30
8.3 Preparatory conditions 31
8.4 Test procedure 35
8.5 Acceptance limits 42
8.6 Quality assurance 43
8.7 Abbreviations and definitions 44
8.8 Dimensions, Forms 47
9 Annex C – “Cold weld data” base (Summary charts) 49

1 Introduction

1.1 COLD WELDING FAILURES

Spacecraft subsystems contain a variety of engineering mechanisms which exhibit ball-to-flat surface contacts. These may be periodically closed for several (thousands of) times during on-ground testing and operational life of the spacecraft. These contacts are usually designed to be static, but in reality they are often subjected to impact forces. Other static contacts are closed without impact, but will be subjected to fretting during the launch phase, during deployment of arrays but also in service life of the spacecraft. In the latter case, the origin may be vibrations of the spacecraft caused by gyros or motion of antennas.
In most cases metals are used in the construction of these mechanisms, preferably light metal alloys, but these are strongly prone to adhesion. Impacts and fretting occur also in terrestrial applications, but the main difference in space is the missing atmosphere (oxygen).

On ground it is unusual to witness any adhesion between either metallic interfaces independent whether they are subjected to impact or fretting. This is because the surface are re-oxidised after each opening. Hence, the next closing is made on new oxide layers. In space, the oxide layers are broken irreversibly. Therefore, the following closing is metal-metal-contact thereby enabling welding effects. These effects may in open literature also be referred to as sticking, stiction or adhesion. Regarding ESA space mechanisms and standardisation the relevant source is [1], using the item “separable contact surfaces”

An **impact** during closing can eventually degrade the mechanism's surface layers whether they are natural oxides, chemical conversion films or even metallic coatings. This can dramatically increase the tendency of these contacting surfaces to "cold-weld". Fig. 1 shows an example for such a mechanism. The anchor was actuated from it’s resting position (middle) electromagnetically, and impacted on both end stops. Finally, an anomaly from the flight model of this mechanism on a satellite was reported, that the anchor kept blocked on the left side (as shown in Fig.1). In technical terms, the adhesion forces were higher than the separation forces available from this mechanism’s spring. Ground simulation of the mechanism in a vacuum chamber led to an adhesion force in the range of 0.3 N. This could be confirmed by impact testing at AIT [2].

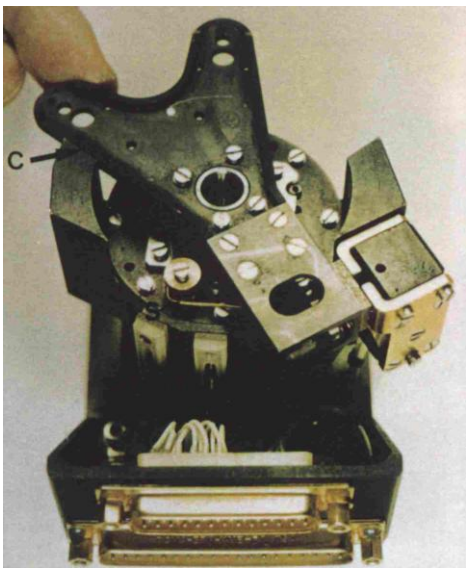

Fig. 1 Mechanism of a satellite: anchor was actuated from it’s resting position (middle) electromagnetically. It impacted on both end stops. Finally, an anomaly from the satellite was reported, that the anchor kept blocked on the left side. It was “cold welded”.

Another even more dangerous effect is **fretting**: vibrations occurring during launch or during movement of e.g. antennas in space, can lead to small oscillating movements in the contact, which is referred to as “fretting”. This lateral motion causes even more severe surface destructions

compared to impact. It may lead to cold welding effects similar to bonding techniques. Adhesion forces may increase to values higher than the closing forces. A failure due to cold welding after fretting occurred on the Galileo spacecraft [3]. The high gain antenna was shaped like an umbrella. Their ribs were locked for launch. The deployment of the high gain antenna could not be fully reached due to cold welding (1991). Investigations have shown that fretting during transport and lift -off caused cold welding of ribs in the launch lock position.

1.2 OBJECTIVE TO SETUP TEST METHOD

“Cold welding” was diagnosed to be the cause of some spacecraft mechanism failures in the late 1980’s and early 90’s. It was clear that some laboratory testing was needed in order to assess the effect of different surfaces making “static contact” under vacuum.
This was done by constructing two dedicated equipments: the "impact facility" and the “fretting facility”. Both were developed at AIT and have been used to investigate several combinations of bulk materials and coatings for their tendency to "cold-welding". The test philosophy is based on repeated closing and opening of a pin-to-disc contact. In an impact test, in each cycle, the contact is closed by an impact with defined energy (no fretting applied). During a fretting test, the contact is closed softly (without impact), and while being closed, fretting is applied to the contact. For both tests, the adhesion force, i.e. the force required to re-open the contact, is measured at each opening. Basic studies [4] were carried out to show the influence of the main parameters impact energy and static load (contact pressure). These first results have been used to set up a standard test method with fixed parameters [5]. In the following sections an overview of the tested combinations is given.

1.3 BACKGROUND TO COLD WELDING EFFECT

Surfaces that are exposed to atmospheric conditions are generally covered by physically or chemically absorbed layers. Even in the absence of absorbed water, grease or other macroscopic contaminants there remain surface layers, such as oxide and nitride layers, which are formed under terrestrial conditions on pure metal surfaces and which can be regarded as natural protection layers against cold welding.
Under vacuum or in space environment, once removed by wear, these layers are not rebuilt and the exposed clean metal surfaces show a higher cold welding probability. So, adhesive and tribological behaviour under space environment or vacuum differs significantly from terrestrial conditions and the use of data collected under latter conditions is rather restricted. Secondly, a modelling of the adhesion forces suffers from the unknown degree of real metal-metal contact, which is linked to the destruction of the surface layers which is strongly affected by the contact situation. Moreover, scientific studies are mostly based on atomically clean surfaces. Hence, the value of adhesion on typical surfaces of spacecrafts produced by “normal engineering“ are somewhere between the high values seen from atomically clean surfaces and the “too low values” which would be derived from “pure static” contact. In a recent study, two theoretical approaches to calculate adhesion forces were compared with experimentally measured adhesion forces for a fretting contact. It was shown, that the modelling approaches cannot predict actual adhesion forces [6].

From general experience [7] and as discussed in previous papers, [8], [4], contact situations may be classified in three different types: static, impact and fretting. In a cyclically closed and opened contact, the amount of destruction of surface layers increases in this order: static, impact and fretting. As surface layers are destroyed we see an increase of the adhesion forces. Fig. 2 shows three plots of the adhesion force as function of cycles (=openings). The three plots refer to three contact types applied to a pairing of titanium alloy (IMI834) and Stainless steel (AISI440C) [8]. In fretting conditions the maximum adhesion force during the whole test was 9.5N (2.5 times the load of 4 N), under impact 0.96 N (load 29 N), whereas in static contact after 25.000 cycles adhesion of less than 0.1 N occurred (29 N load). A theoretical deduction would have given an estimate of 7.7N without any relation to the real contact situation: Hertzian contact area 0.006mm² times yield stress of this Ti-alloy (~1200MPa).

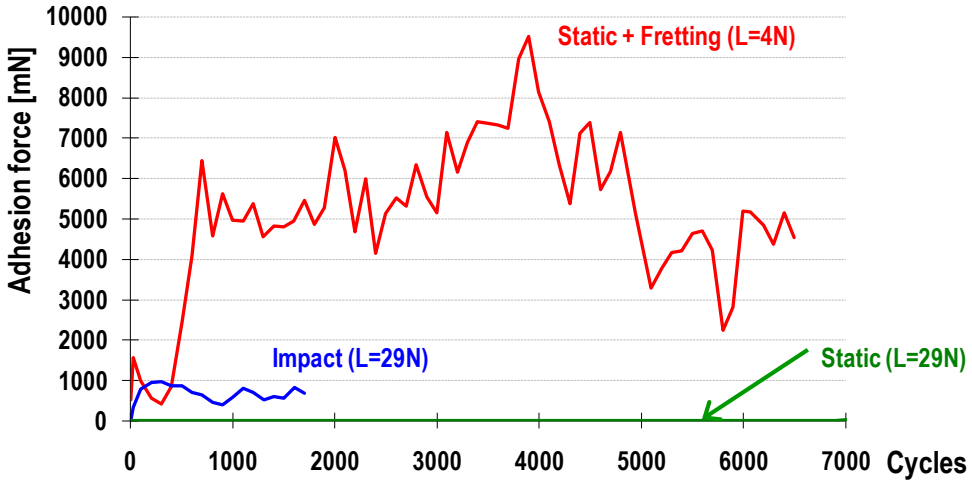

Fig.2 Adhesion force as function of cycles (i.e. one closing-separation) [8]. Comparison of adhesion in static (load 29N), impact (load 29N) and fretting (load 4 N) condition under vacuum. Danger and severity of adhesion increases with contact: static- impact – fretting. (Max. adhesion in static 0.1 N after > 25000 cycles, in impact 0.96 N, in fretting 9.5 N.)

Summarising, contaminant layers (oxides) are removed under impact and fretting much more quickly as compared to static contacts, and cold welding occurs much earlier than expected. This may not only reduce the life time of a satellite but also can endanger space missions, e.g. any opening or ejection mechanism may fail due to cold welded contacts. A typical opening/closing mechanism can fail, if the adhesion force exceeds the force which is available to open this mechanism, e.g. by a spring. This ”blocking“ value may be much lower than the applied load. The blocking of the mechanism (Fig. 1) under impact condition was reported with an adhesion force in the range of 0.3 N. This value was confirmed by a first verification study of the impact device [2].

2 Cold welding test method

The test method reported herein is based cyclic contacts. A pin is pressed onto a disc for several thousand times. At each opening the force required to separate pin and disc is measured. This force is referred to as “adhesion force” of this cycle. The adhesion force is plotted as function of cycles. Comparison of different materials is based on the maximum value of adhesion found during a whole test.
To enable comparison of cold welding tendency between different material pairings, the following testing philosophy was set-up at AIT (it is described in detail in an in-house specification of AIT [5]): the parameters static load and impact energy are fixed for each pairing with respect to elastic limit (EL) of the contact pairing. Hertz' theory is used to calculate to contact pressure in the ball-to-flat contact. Using the yield strength of the softer material, the "von MISES-criterion" defines an elastic limit (EL): if the load (contact pressure) exceeds this EL, plastic yield would occur. Similarly, for the impact energy a limit (W_Y) can be deduced above which yielding occurs [5], [9]. Based on parameter studies [8], [4], an AIT-standard was defined and approved by ESA: the static load is selected to achieve a contact pressure of 40, 60 and 100%EL. An impact test is started with a static load, which achieves 40% of EL. After 10000 cycles, the load is increased to achieve 60%EL. After, another 5000 cycles 100%EL are applied. The impact energy is kept constant to 40 times the W_Y. This stepwise increase of load enables to continually obtain data during one test run. (From the point of possible irreversible plastic deformations, loads may be increased but must not be decreased. In the latter case, work hardening of material might have increased hardness, and therefore the actual contact pressure is lower than calculated.) For fretting tests, only one static load (related to 60%EL) is applied for 5000 cycles. Fretting parameters are a stroke of 50µm at a frequency of 200Hz. Uncoated specimen are freshly ground to a surface roughness of Ra<0.1µm before testing [5]. The contact is closed for 10 seconds and then and opened for 10 seconds, too. At impact the base pressure of vacuum was less than 5.10^{-8} mbar, i.e. surfaces are not recovered during opening. During fretting test, a base pressure of 5.10^{-7} mbar is sufficient, since the change from oxidative wear to adhesive wear is in a range of 0.1 to 10^{-3} mbar. (The devices are described in Annex A, a detail of the fretting test equipment is shown in Fig.3.)

The European Co-operation for Space Standardisation (ECSS) has released specifications on contact surfaces. In the ECSS-E-ST-33-01C Rev.2 Mechanisms, section 4.7.4.4.5 “Separable contact surfaces” [1], following main requirements are stated:

b) Peak Hertzian contact pressure shall be below 93% of the yield limit of the weakest material. (This refers to a contact pressure of 58% of the elastic limit, EL.)
d) ... the actuator shall be demonstrated to overcome two times the worst possible adhesion force ..

Therefore, results obtained from cold welding tests acc. to the ARCS-in-house-specification [5], can be used to address the necessary opening forces for actuators in mechanisms. (Both, impact and fretting test are done at 60% EL.)

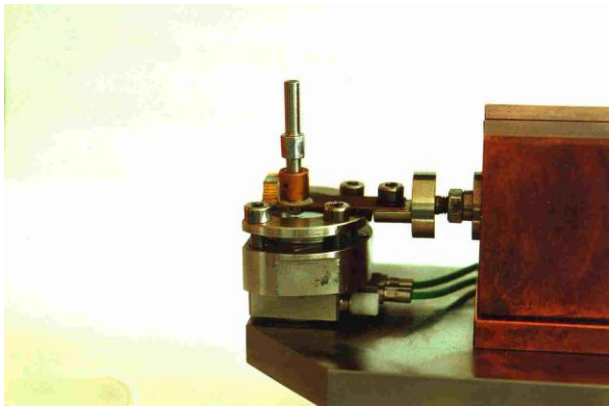

Fig.3 Fretting device: Detail showing the fixation of pin (upper rod) and disc (mounted directly on a force transducer). Right side: piezo actuator for generation of fretting movement.

A full description of the test equipment is given in Annex A. The test method [5] and the specimen geometries are given in Annex B. Several tests have been performed since the test method was standardised and those results have been compiled in Annex C. (Actually, data of Annex C can be obtained via a WEB-based data base: https://coldweld.aac-research.at/ .)

3 State of the art (ESA published data)

In this section knowledge in the field of cold welding is overviewed. It covers on one hand test results related to materials' and coatings' behaviour divided into impact and fretting. On the other hand, also some more general aspects like influence of contact parameters on adhesion.

3.1 RESULTS ON IMPACT

3.1.1 Typical space materials under impact

In the following, comparison of data will be based on the worst case of impact (100%EL). A table, compiled in Annex C details the materials and the abbreviations used. A survey of adhesion forces found for a selection of typical (uncoated) space materials is shown in Fig. 4. Highest adhesion is seen for stainless steel SS17-7PH versus itself (Fig.4) or Al AA 7075 versus itself (1744 mN). This is an unexpected experience, since usually titanium is regarded as the most "dangerous" contact material. From a crystallographic point of view, face centred cubic metals are the most prone to adhesion: Fe, Al. This is due to their high ductility. A study [10] on the adhesion of different working materials to a cutting tool made of high speed steel indicated a relation between adhesion force and Ni-content. Regarding standard tests made with different steels to themselves, results show that the standard bearing steel (AISI 52100) has negligible adhesion. For the AISI440C (no Ni) certain adhesion under impact was found. Mixing of steels can reduce adhesion. (Fig.5.)

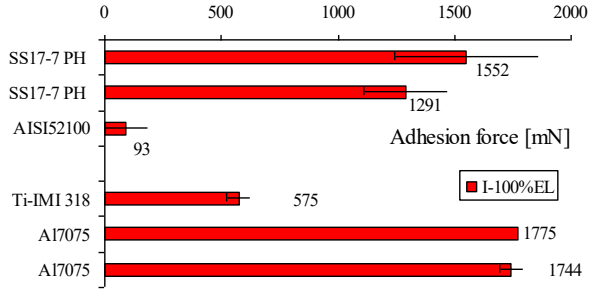

Fig.4 Adhesion force under impact for materials in contact to themselves. Highest adhesion for stainless steels with Nickel (e.g. SS17-7PH), and Al alloys (Al AA7075). Medium adhesion for Ti-Alloy. Low adhesion for bearing steel AISI 52100 (no Ni).

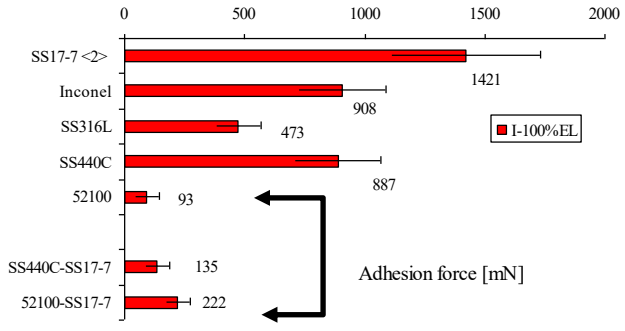

Fig.5 Adhesion force under impact for different types of steel versus itself: austenitic structure and Ni seem to promote high adhesion: SS17-7ph (7%Ni), AISI 316L (11%Ni), Inconel 718 (52%Ni). No adhesion for AISI52100 versus itself ("52100"). High adhesion of AISI440C has to be proven. Combinations of different steels: adhesion seems to increase in contact to steels with higher tendency to cold welding (arrow).

3.1.2 Influence of coatings on steel

Stainless steel discs (SS17-7PH) were coated with TiC and MoS_2 and investigated for their ability to reduce adhesion. These coatings are related to two types of coatings: respectively hard and soft. The efficiency of the first group - **hard coatings** - depends on the load bearing capacity of the underlying bulk: if it is too soft, it is deformed under impact, and the hard coating breaks [11]. Then the underlying metal comes into contact to the metal of the opposite metal surface, and adhesion is found. However, pieces of the hard coating (TiC) are still present. They may be transferred and may act as additional abrasive particles. Hence, adhesion may be decreased in comparison to bare metal surfaces, but since destructed surfaces areas cannot be „re-coated“ adhesion still occurs. An example for this is the **TiC** (2000 HV) on the SS17-7PH (only 441HV): the coating decreased the adhesion force by about four times, after the TiC brake-off it was no longer effective and a marked increase in adhesion force was measured.. (See Fig.6.)

Hence, a hard coating should be applied on steel types which enable a higher hardness, e.g. AISI440C or AISI52100 (up to 700 HV). This would avoid plastic deformations of the underlying steel substrate, which results in cracking of the coating.
Instead of using a hard coating, a harder steel type may be selected for contact to stainless steel SS17-7PH. By use of steel AISI52100 in contact to SS17-7PH lower adhesion can be achieved (222 mN, Fig.5). This can further be reduced by application of hard coating on hard steel: DLC by VITO [12]. (Fig.6.) The hard **DLC-film** did not (visible) peel off and no adhesion during more than 37.000 cycles was measured. Some small amount of steel was transferred from the (un-coated) pin to the DLC-coated disc. Before selecting DLC, great care has to be put on it’s composition. Most of conventional DLC coatings are not compatible with vacuum applications.
Secondly, a **soft lubricant** coating on SS17-7PH could avoid any adhesion to another SS17-7PH pin. Hence, under impact soft lubricant coatings on stainless steels reveal higher efficiency in prevention of cold welding than hard coatings.

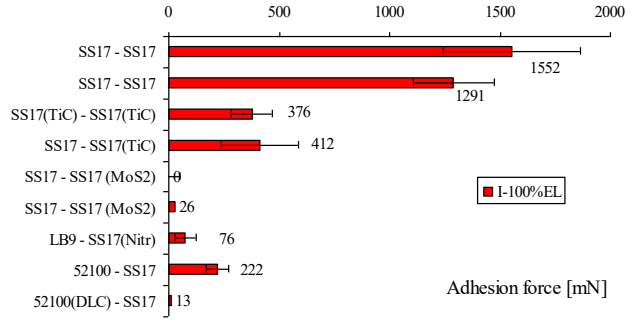

Fig.6 Adhesion force as function of static load for different coatings on steel: lowest adhesion for SS17-7PH (SS17) with MoS2. Higher adhesion for TiC (coatings were broken). Negligible adhesion between bronze (LB9) and SS17-7PH (LB9-SS17(Nitr)). Low adhesion between AISI52100 and SS17-7PH, can further be decreased by use of DLC coating (“52100(DLC)-SS17”).

3.1.3 Influence of coatings on aluminium an titanium

On the other hand, (hard) **finishes on the soft aluminium** showed breaking and removal of the upper layers, but did not enable cold welding. Tests were run up to 50.000 cycles without finding sudden increases of adhesion forces. Fig. 7 shows a comparison of the maximum adhesion forces of Al AA7075 versus itself (uncoated: Al7075-Al7075) and the influence of selected coatings. No adhesion was found for combinations: Al AA7075 hard anodised versus stainless steel SS15-5PH (“Al7075(anod)-SS15”) and Al AA7075 CrNi-coated versus Al AA7075 hard anodised (“Al7075(CrNi)-Al7075(anod)”). However, an Alodine 1200 coating only on the disc is not sufficient to prevent adhesion (Al7075(alod)-Al7075, adhesion force of 336mN).
A recently developed coating, named “Keronite”, did not show any adhesion, too. But the main advantage was that no surface destruction or formation of debris was found. (For details to Keronite refer to [13].)

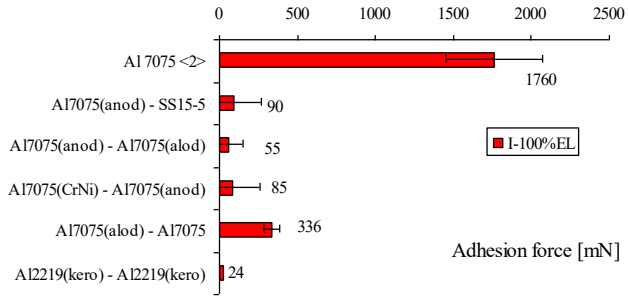

Fig.7 Maximum adhesion force under impact for different coatings on aluminium (AA7075): negligible adhesion for combined coatings "Hard anodised (anod)", CrNi-plated (CrNi), Alodine 1200 (alod) and Keronite [13], Alodine alone is not sufficient to prevent cold welding (336mN). (For details on Keronite coating refer to [13].)

Coatings on **Ti-alloys** show under impact can be divided in two groups: solid lubricants like MoS_2 or Dicronite DL5 (WS_2) do not prevent cold welding on Ti-alloys. Hard coatings like Dicronite+, Balinite or Keronite do. (Fig.8.)

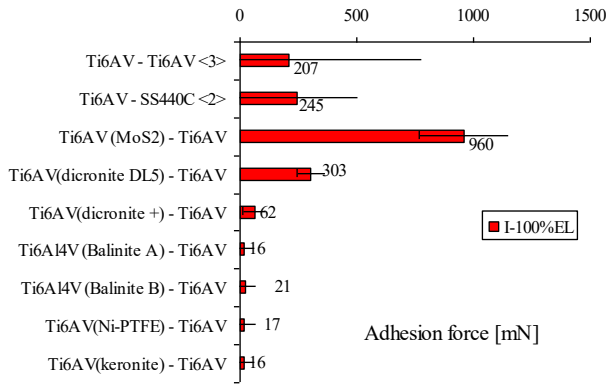

Fig.8 Adhesion force under impact for different coatings on ti-alloy: hard coatings coatings provide good prevention of cold welding, solid lubricants only fail (MoS_2, WS2).

3.1.4 MoS_2 coatings versus MoS_2 composites

The investigations included also two composites materials containing MoS_2 particles: Vespel SP3 (Polyimide with 15m% of MoS_2) and a silver alloy "$AgMoS_2$" (with 15v% MoS_2). Vespel shows negligible adhesion against both, stainless steel SS17-7PH and Al AA7075. The silver alloy shows some small adhesion 117 mN. (The combination Ag10Cu versus $AgMoS_2$ is used in slip rings.) SEM-inspection showed the counter-surfaces (partially) to be covered with MoS_2 flakes, which were pressed out of the matrices. This effect is assisted by the fact that adhesion is mainly driven by bonding between two metals. In case of Vespel SP3 no metal is present. In case of silver, the very low shear strength enables easy braking of the bonds. Hence, beside coatings also composites provide efficient prevention of cold welding, due to their ability to re-form, i.e. at each impact a new lubrication layer is formed and coating free areas are re-coated. (Fig. 9.)

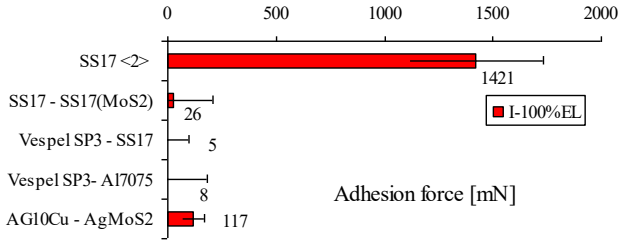

Fig.9 Adhesion force under impact for different combinations with MoS_2: coatings and composites provide good prevention of cold welding (SP3 = Vespel SP3, Ag10Cu = coin silver, $AgMoS_2$ = silver composite with 15v% MoS_2) .

3.2 RESULTS ON FRETTING

3.2.1 Comparison of impact and fretting contact

A survey of adhesion forces found under fretting and under impact is given in Fig.10. (Data from [12], [14], [15], [8],[16].) As mentioned in the Introduction, the fretting movement which is a small sliding, was expected to cause sever surface destructions. In highest allowed contact pressure at impact (100%EL), typical adhesion forces range up to approx. 2000 mN. Under fretting conditions at even lower contact pressure (60%EL), the adhesion forces exceed these values by factor of up to 10. Stainless steel SS17-7PH versus itself shows adhesion of approx. 1500 mN under impact, but more than 11000 mN in fretting (Fig.10 "SS17-7"). For other metal-metal contacts similar behaviour is found, Al AA7075 versus itself [15]. The highest adhesion was found for Inconel 718 (Ni alloy). No adhesion is found for polymer to metal contact, e.g.VESPEL SP3 (polyimide with 15m% MoS_2) versus stainless steel SS17-7 PH.
As mentioned earlier, the adhesion of different construction steels to a cutting tool made of high speed steel indicated a relation between adhesion force and Ni-content in fretting conditions [10]. Standard fretting tests [5] done on different steels versus themselves, also show this basic relationship (Fig.10). Adhesion decreases in the order Inconel 718 (52%Ni), SS17-7PH (7%Ni) and AISI 316L (11%Ni), down to AISI 52100 and even lower for AISI440C (no Ni). The bearing steels (AISI 52100 and SS440C) show lowest adhesion under fretting. (The high adhesion of the AISI440C (no Ni) under impact is still under investigation.)

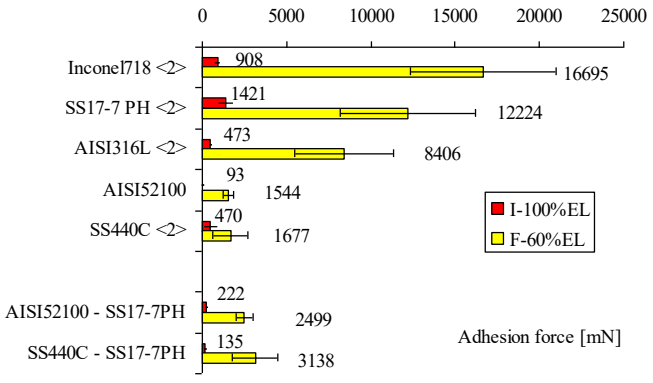

Fig.10 Comparison of adhesion force under impact (I) and fretting (F) for different steels and Ni-alloys versus themselves: Fretting initiates higher adhesion, for ferrous alloys adhesion decreases with decreasing content of Ni as indicated by [10]. Combinations of different steels seem to be dominated by the one with higher adhesion: AISI52100 to SS17-7ph. (52100-SS17)

3.3 INFLUENCE OF COATINGS ON FRETTING

3.3.1 Coatings on steel

The previous Section has shown that certain alloys exhibit high adhesion. Therefore, typical coatings were investigated for their ability to prevent cold welding under fretting. Results for **coatings on steel** are compared to contacts of bare materials in Fig.11. Applying a **MoS_2 coating by PVD** to one of the two SS17-7PH counterparts could not prevent adhesion: in two tests after only 50 (20) cycles, i.e. 8 (3) minutes fretting or 100000 (42.000) strokes lubrication effect was lost. This is combined with a distinct increase of adhesion force. High adhesion forces of up to 5870 mN were found. This refers to a reduction of the max. adhesion forces of approx. 50 % (compared to SS17-7 without coating). (Fig. 11.) The same tendency can be seen for one **TiC coating** between two SS17-7ph counter parts (Fig.11: "SS17-SS17(TiC)"). Adhesion is only reduced to approx. one third of the uncoated combination. SEM images and EDAX analyses confirm the breaking of the coating and adhesive wear.
The influence of **nitriding** SS17-7ph surface was investigated: no significant reduction of adhesion is visible (still 8517 mN, Fig.11: "SS17-SS17(nitr)".) Based on this result, the low adhesion between nitrided SS17-7 and bronze LB9 (500-1087 mN) may be due to the lubrication effect of the lead (known for tribological applications).

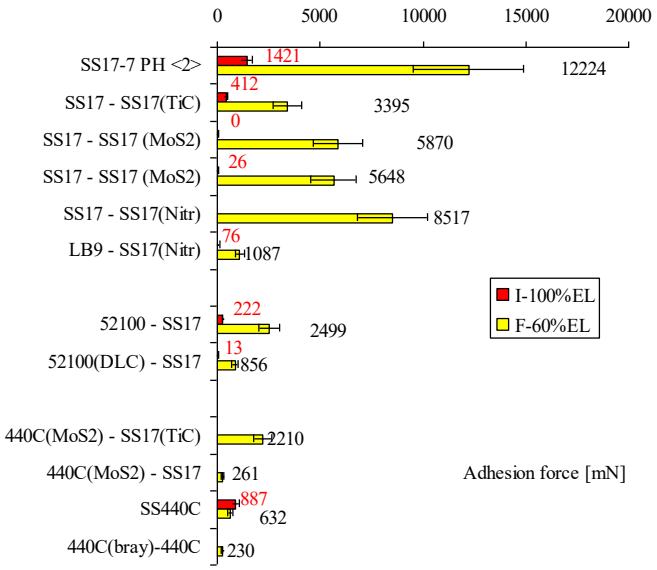

Fig. 11 Adhesion force of steel based coatings (I=impact and F=fretting): coatings in general reduce adhesion. For SS17-7PH no tested coating of the disc could decrease adhesion significantly (TiC, MoS_2 or nitriding). In contact of AISI440C to SS17-7ph, TiC shall be avoided. Efficiency of grease (Braycote601) is not significant in contact of AISI440C to itself. Efficiency of MoS_2 coating under fretting is limited to a low endurance.

Applying a **DLC coating** on AISI52100, reduces adhesion in contact to SS17-7ph from 2499 mN to 856 mN.
The effect of **grease** (Braycote 601) was tested in a contact AISI440C to itself. No significant effect is visible. Hence risk of contamination due to outgassing is superior to the efficiency in avoiding adhesion. (Fig.11: "440C(bray)-440C".)

MoS_2 coating in a special pairing (AISI440C+MoS_2 vs. SS17-7PH+TiC): MoS_2 + TiC resulted in a breakthrough (at 366 cycles = 61 minutes = 700000 strokes) and medium adhesion forces of up to 2210 mN. Applying only MoS_2 on a AISI440C disc and performing test versus SS17-7PH only very low adhesion forces were found. (Compare AISI440C vs. itself without coating, Fig.11: "SS440C".) Therefore the conclusion could be drawn that the TiC destroys the surface layers of the AISI440C which could have been regarded as adhesion prevention layers.

3.3.2 Coatings on aluminium and titanium

Selected combinations of coatings on **aluminium** were tested under fretting: no adhesion was found between Al AA7075 hard anodised and Al AA7075 NiCr-plated. (See Fig. 12.) Al AA7075 hard anodised in contact to non-coated SS15-5PH showed negligible adhesion. This is in contrast to the fact, that SEM-images show breakthrough and pealing off of the conversion layer on the Al. But results are in accordance to impact tests done in [14]: despite of a breakthrough of the layer, no adhesion was measured. Coating of only the disc with Alodine, did not prevent from cold welding, medium adhesion of 2036 mN was found. (Fig.12: "Al7075(alod)-Al7075") Alodine1200 is a chemical conversion coating composed of hydrated aluminium chromate which is very thin (<1µm). Therefore, the fretting wear resistance is very low and the coating was broken setting free the aluminium metal beneath.

In contrast to this very thin conversion layer, very thick ceramic like coatings may be obtained on aluminium and titanium by Plasma-Electrolytic-Oxidation process (PEO). Such a coating on aluminium may reach thicknesses up to 100µm [13], [17]. For space applications thickness in a range of 10 to 30µm would be of interest. Such a coating developed by "Keronite" was in a first study screened. It offers not only no adhesion to steel AISI52100, but also did not peel off during fretting [18]. (A later study has confirmed this, see section 3.4 [19].) This is an advantage to anodised layers, where debris is produced which could contaminate other areas in the space craft.

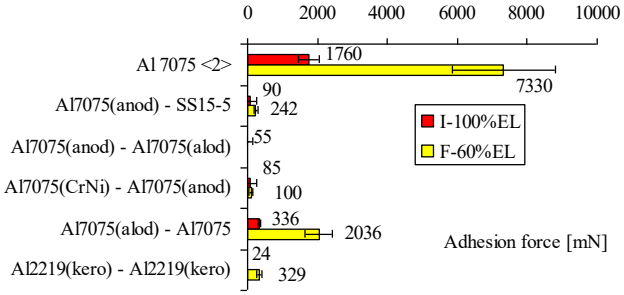

Fig. 12 Adhesion force of aluminium based coatings (I=impact and F=fretting): Adhesion between Al parts is strongly reduced by hard anodising (anod), CrNi-plating (CrNi), no adhesion for (thick) Keronite [13],[18]. A single Alodine coating (alod) is not efficient in prevention of cold welding, because of it's low thickness <1µm.

Another often used alloy is **titanium alloy Ti6Al4V** (Ti6AV). Since, titanium has also high affinity to cold welding, several coatings were investigated. In a first study, only the disc was coated and the Ti6AV-pin was left uncoated. Herein, all of the coatings were broken and adhesion was found before end of the test (5000 cycles). Moreover, no clear recommendation towards soft or hard coatings can be deduced. The lowest adhesion values were found for Balinite B and a thin version of Keronite for titanium (6µm), but also for the solid lubricant Dicronite DL5. (Fig.13.)

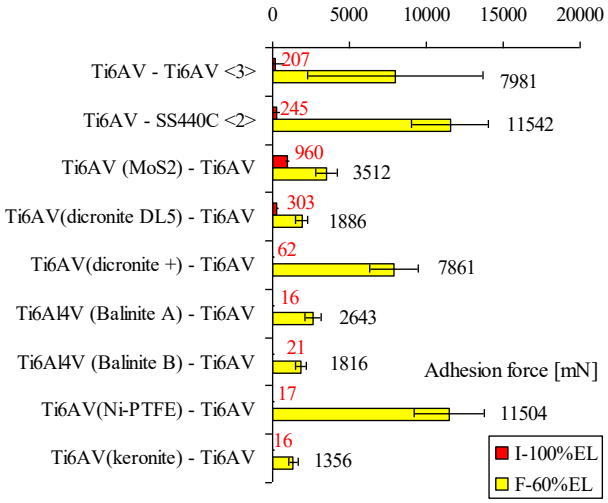

Fig. 13 Adhesion force of coatings on Ti6AV (I=impact and F=fretting): under impact hard coatings prevent cold welding, under fretting all coatings were broken, lowest adhesion for Balinite B and Keronite (thin ~6µm).

3.4 THIN AND THICK COATINGS UNDER FRETTING AND THERMAL CYCLING

It can be seen in the results above, that long term fretting testing of hard coatings on softer substrate metals led in most cases to failure of the coating. Examples are TiC on stainless steels [15], anodising of aluminium alloys [12] or several coatings on Ti-alloys [16]. For all these coatings one common parameter is their thickness: it is in a range of a few microns.

A dedicated set of studies was done to investigate if thick coatings are more resistant to cold welding under fretting conditions. The 3G Keronite process enables to achieve thick ceramic coatings on soft metallic substrates. It is based on Plasma electrolytic oxidation (PEO). This is one of relatively new environmentally safe electrolytic coating processes, applicable to light metals like Mg, Al, Ti and their alloys. It represents a rapidly developing sector in surface engineering. The process involves the use of higher voltages than in anodising and the electrolyte usually consists of low concentration alkaline solutions and all variants of this process are considered to be environmentally friendly. The process results in the formation of ceramic layers with thicknesses up to 100µm.

Therefore, coatings with thickness from 17 to 55µm were applied three common aluminium alloys (AA2219, AA7075 and AA6082) widely used in spacecraft hardware. They were investigated for their resistance to cold welding under fretting before and after thermal cycling. As counter part conventional bearing steel AISI52100 was used. No adhesion could be found and the coating did not break. Then the coatings were subjected to 20 thermal cycles between -185 and +107°C no cracking/delamination was detected after that. Finally, again fretting test were done: again the coatings survived without showing breakage, debris formation or adhesion [19]

Hence, 3G Keronite coatings with ~20µm on aluminium in contact to bearing steel do not show breaking of the coating or adhesion in fretting. On the other hand, Keronite coatings with thickness of 6-10µm on Ti-alloy Ti6Al4V was found to be no sufficient to prevent cold welding. In contact to itself or to INVAR breaking was identified and cold welding occurred. However, for Keronite in contact to itself with one additional layer of MoS2 (PVD) no cold welding was found. [20], [20]. This study also considered thermal cycling, even down to liquid helium: no degradation due to thermal cycling was found by metallographic inspection and by second fretting tests.

Following these studies, thick Keronite coatings (>17µm) offer really enhance resistance against cold welding under fretting and ARE NOT degraded by thermal cycling. The role of mos2 coatings (resin bonded or PVD) on top of Keronite has still to be investigated in more details: in some cases no additional benefit can be found, but at least no drawback is known yet. [20], [20], [19].

3.5 SURFACE MORPHOLOGY AFTER IMPACT AND FRETTING

Surface is strongly changed due to impact and fretting. After impact testing, a SS17-7PH pin shows plastic flow, which can be seen by the piling up at the edges of the pin's contact area (Fig.14a). On the other hand, fretting of a SS17-7ph steel versus itself shows strong surface destructions due to adhesive wear. Material is torn out of the surface, and pressed back or adheres to the contact partner. (Fig.14b)

As mentioned above, MoS_2 coating on SS17-7PH could not prevent from cold welding. The lubrication effect was lost after 20 cycles (200 seconds fretting, 42000 strokes). Afterwards, adhesion up to 5870 mN was found. Fig. 15 shows strong surface destruction of the MoS_2 coated disc, which is similar to the uncoated. EDX-distribution of Mo taken from the disc shows, that no Mo is present in the contact area after 7000 cycles. Both, pin and disc, show fretting wear scars which are similar to those without MoS_2 coating.

In contrast to all coatings investigated until now, the thick Keronite on Al AA2219 was the only one which prevents adhesion and which was not destroyed under fretting conditions. Hard anodising of Al AA 7075 prevented adhesion, but much loose debris was found. (Fig. 16.)

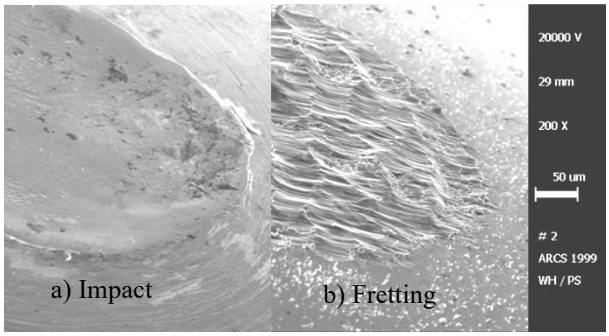

Fig. 14 Surface of a pin (SS17-7ph) after impact and fretting. Impact: only some plastic flow visible by piling up of edges. Fretting: strong destruction of surface, adhesive wear combined with high adhesion forces (Compare to Fig.10 for adhesion forces: "SS17-7".)

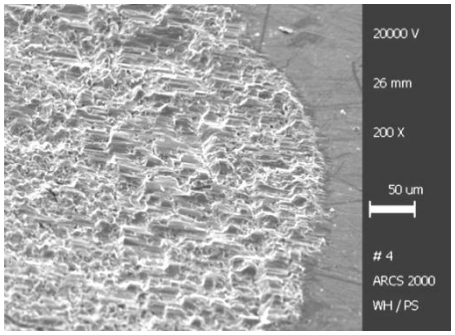

Fig. 15 Surface of disc SS17-7ph with MoS_2 coating after fretting tests (compare to Fig. 11 for adhesion forces): lubrication effect was lost after less than 200 second fretting movement (confirmed by EDAX-mapping: no Mo present in contact area).

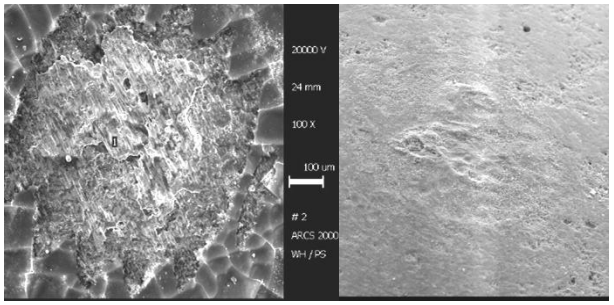

Fig. 16 Comparison of Al-coatings under fretting: Left: Hard anodising on Al7075 was broken. Right: Keronite coating on Al AA 2219 does not show fretting marks. (Compare to Fig. 11 for adhesion forces).

3.6 INFLUENCE OF CONTACT PARAMETERS ON FRETTING / THEORETICAL PREDICITON OF ADHESION FORCES

3.6.1 Background – Influence in Impact contacts

Basic studies [11] by AIT have shown that under impact conditions, an increase of the static load lead to an increase of the adhesion force. Fig. 17 shows the adhesion forces found for stainless steel SS17-7ph in contact to itself (ball on flat contact, without any coating). The three bars refer to the measured adhesion under static loads related to contact pressures of 40, 60 and 100% of the elastic limit. It can be seen that the adhesion forces increases with the contact pressure, when impact occurs (no fretting).

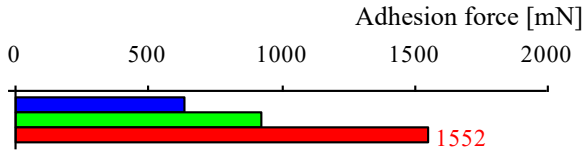

Fig.17 Adhesion forces (in mN) of steel SS17-7ph versus itself (uncoated) under impact, adhesion increases with static load, i.e. contact pressures 40-60-100%EL

On the other hand, studies investigating adhesion under fretting have shown strongly severe wear. (See above.) Impact leads only to some plastic deformations, leading to adhesion forces not higher than 2 Newtons. Fretting, however, causes severe surface damages leading to adhesion forces of several sometimes more the 10 Newtons. Hence, for fretting this influence has to be assessed separately.

3.6.2 Simulation of contact area – Definition of "REAL CLEAN CONTACT AREA"

Up to now, the influence of "material" on adhesion forces was discussed. But cold welding does not only depend on material, but also on geometry namely, the contact area. The macroscopically measureable adhesion force is defined by the following basis: ultimate yield strength (of the softer material) times "real clean contact area". Here, the latter is generally unknown, unpredicatable and orders of magnitude smaller than expected. In the following we use following "contact areas":

1. Nominal contact area
2. "Real contact area"
3."Real clean contact area"

1. **Nominal contact area:** As typically for tribological contacts in mechanisms, only the nominal contact area is known. In flat-to-flat contacts the "nominal contact area" is obvious, in ball-to-flat-contacts it may be calculated by Hertzian theory assuming the contact to be within the elastic regime.
2. **"Real contact area":** Due to roughness not the full contact area comes into contact, only the tips will be in contact. Of course this share between nominal and real contact area is influenced by mechanical and surface properties. In general, this real contact area is by orders of magnitude smaller than the nominal one. Some strategies exist to estimate this "real contact area": Archard has proposed an analytic way to estimate the real contact area: divide the load by the yield strength. Modern computational tools may be used to simulate real contact areas using 3D-topographies and mechanical data. However, this is still only practicable for static contacts. Including motion leads to increased computational efforts.
3. **"Real clean contact area":** In order to calculate adhesion forces, one more reduction step is necessary: again only a part of the real contact area contributes to adhesion. As mentioned earlier, surfaces are covered by natural contaminant layers. Especially, chemical reaction layers prohibit the cold welding. If the tips of two rough bodies come in to contact, both of these layers must be broken in order to enable a metal-to-metal contact. Only this "single joints between the clean metal surfaces are welded", and adhesion force is the sum of all these single welded joints. Finally, it is this last contribution which cannot be predicted anyhow by simulation.

Hence, it must be anticipated that a theoretical prediction of adhesion forces is not possible. Moreover in case of fretting, wear would have additionally to be considered, since it changes the surface topography and the contact area. In order to prove theoretical and experimental approaches, a study was performed [6].

3.6.3 Determination of adhesion forces 3 approaches (models and experiment)

The objective of this study was to investigate if contact pressure and contact area have an influence on the adhesion force under fretting conditions.

Therefore, a set of 4 test parameters was selected with varying load and pin radius (i.e. curvature of spherical pin tip). Table 1 shows the test parameters. Three tests were done at load of 1 N with radii of 1, 2 and 15mm. This is related contact pressures of 118, 57 and 19% of the elastic limit. One test was made with similar contact pressure of 58%EL, but using a different combination of radii (10mm) and load 12N. (See Table 1.) For all tests the same material combination was selected: AISI316L in contact or itself without any coating. This is a stainless austenitic steel, which was already tested previously and shows high adhesion forces. Three parallel tests were done for each set of parameters. (For materials properties refer to table in annex. The calculations of contact pressures were done using standard Hertzian theory, see e.g. [9].)

Table 1: Test parameters: three parallel tests per set

Tests	Tip Radius mm	Load N	Contact pressure MPa	Contact pressure in % EL	Contact area [mm2]
F1x	1	1	1272	118	0.0012
F2x	3	1	611	57	0.0025
F3x	10	12	209	58	0.0287
F5x	15	1	627	19	0.0072

Theoretical estimation of adhesion forces (Approach 1 “Theory”)

Theoretically, adhesion forces could be calculated on following basis: ultimate yield strength times contact area. Whereby, the contact area of ball-to-flat-contacts is calculated using Hertz theory. Following that, the adhesion forces in a ball-on-flat contact should decrease when using a smaller contact area. The values for the stainless steel AISI316L versus itself are shown in Fig.18. It can be seen that, the (theoretical) adhesion force is directly related to the contact area (Table 1).

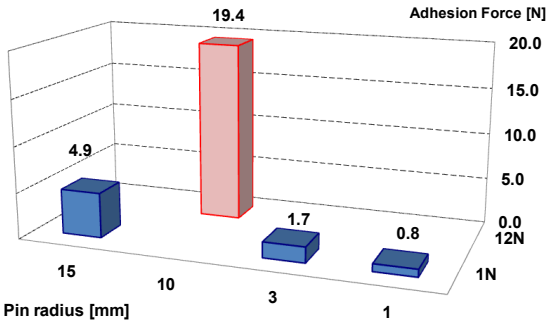

Fig.18 Adhesion forces: calculated using Yield strength times Hertzian contact area.

Estimation of Adhesion forces using fretting wear area (approach 2 “Semi-Theory”)

A second way to predict adhesion forces might be based on experimentally derived contact area: use the measured wear contact area after a friction test and multiply it with the yield strength. The results are shown in Fig.19. Here, the contact area measured after the fretting tests were multiplied with the yield strength.

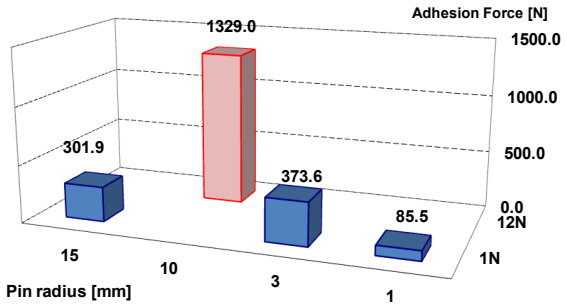

Fig.19 Adhesion forces: calculated using Yield strength times wear contact area, i.e. the contact area measured after the fretting test.

Results from fretting experiments (approach 3 “Experiment”)

For each set of parameters three parallel tests were done. Averaged values for each set of parameter are shown in fig.20. Adhesion forces are generally high but expected for this material. The only significant difference is seen for the smallest contact area (pin radius 1mm at 1N). Here the adhesion force is slightly lower (6.2N).

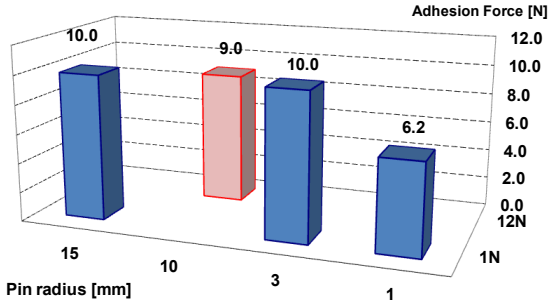

Fig.20 Adhesion forces: measured values (average value of three parallel test, uncertainty of test method 30%).

On the other hand, fretting wear leads to an increase of the contact area. The contact area of the test with the higher load is remarkably higher than the other tests. Hence, wear is higher for higher loads, even if the contact pressure is comparable: ~58%EL similar for radius of 10mm and load of 12N to radius of 3mm and load of 1N.

3.6.4 Comparison of modelling and experimental results from fretting

Adhesion under fretting was derived by three methods:

1. **Theory:** calculation by yield strength times Hertzian contact area, this would lead to the conclusion that smaller radii are preferable. Neglecting any wear, Hertzian theory gives a smaller contact area. The resulting adhesion force is accordingly lower. (Fig.18.)

2. **Semi-Theory:** yield strength times measured wear contact area, i.e. use of the wear contact area which is measured after a fretting test (Fig.19). The derived values for the adhesion force are similar to approach 1. The conclusion would be similar to the approach 1-Theory: use smaller radius. Even though the contact pressure is higher than the EL, the wear does lead to a smaller contact area when the tip radius is smaller. However, starting with contact pressure higher than EL is still no issue.

3. **Experiment:** measured adhesion forces are quite comparable for all parameter sets. They do not show significant influence of initial contact details (fig.20). Smaller contact radius seems to be advantageous, the adhesion force is slightly lower (average 6.2N compare to approx. 10N for all other tests).

It is clearly visible that both theoretical and semi-theoretical extrapolations do not fit to the experimental behaviour. The main reason is seen by fact that the definition and determination of the "contact area" is insufficient: the theoretical approaches reveal a "nominal contact area", but the adhesion is related to what shall be referred to as "real contact area":
The real contact area, i.e. the area where metallic bonds actually exist, is much smaller than the nominal one predicted by theory. This is due to the surface roughness and the surface contamination. Both factors reduce the measured adhesion forces by orders of magnitude (compare Fig.19 and 20). Using theoretical approaches, at a load of 12N the highest adhesion should be found (Fig. 18 and 19.). Even this overall tendency is not found in experimental testing (Fig. 20). Wear due to fretting is levelling out the contact pressure to values in a range of few Megapascals.
Hence, adhesion forces cannot be "modelled" since neither the "real contact area" nor fretting wear are predictable.

4 Data base “Cold Weld Data”

4.1 INPUT FOR DATA BASE

Several studies on Cold welding of material combinations were performed in the past years. They were performed according to the ARCS-In-Home-Standard agreed by ESTEC [5] and are therefore regarded as being comparable. (Tests done within separated project or customer projects are not included in this data base.) For each test a data sheet was prepared within the related call off order. From all these performed tests single data sheets were made (see Fig. 21). They have been collected and can be accessed via the WEB [21].

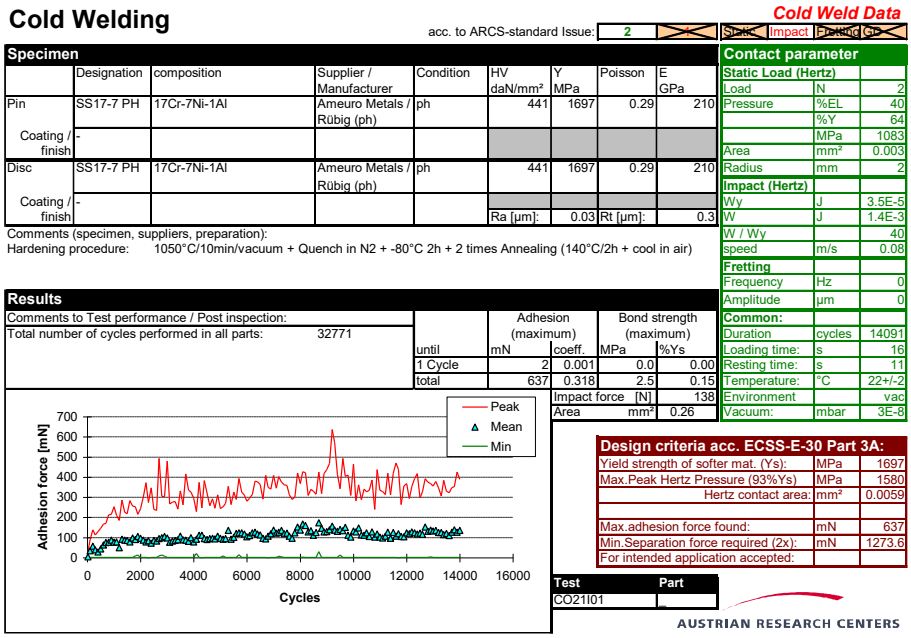

Fig.21 Data sheet generated for each cold welding test cone acc. to In-House-test method [5]. These data sheets are available on Internet.

4.2 CLASSIFICATION OF ADHESION FORCES AND WEB-DATA BASE

They were now collected into an electronic data base. Survey tables were created showing for which combination data is available. It also includes a classification in four levels (Tab.2). Finally, in the electronic version from the survey each data sheet can be accessed.

Based on the result of "General Validation Studies" a data base was initiated:

- Comparable due to test parameters related to material properties
- It covers the contact modes " impact" and "fretting"
- A Summary table shows available material combinations
- For each tests a detailed data sheet is available
- The summary table shows a "classification" related to the severity of adhesion

Related documents:

- The test method is described in ARCS-in-house-specification.
- This includes also sample dimensions and derivation of test parameters.
- The summary of all tests is divided in Fretting and Impact
- For each test a detailed data sheet can be opened (click on symbol)

Classification of material combinations:
The tables are based on following classification:

Table 2: Classification of adhesion forces as sued in the WEB-data base.

Symbol	Adhesion force [mN]		Comment to adhesion	Comment to Use
	lower limit	upper limit		
●	0	200	No or negligible adhesion, noise of test	Use recommended
◑	201	500	Small measureable adhesion	Security measures to be undertaken
◔	501	5000	Strong adhesion	Direct use not recommended
○	5001	higher	Severe adhesion	Direct use not recommended

4.3 WEB-DATA BASE: HOW TO ACCESS AND USE

The database is available the on the website:
Tribological Tests - Aerospace & Advanced Composites GmbH – Consulting, Testing, Development, Research

but also directly:
Coldweld Data Base | Aerospace & Advanced Composites

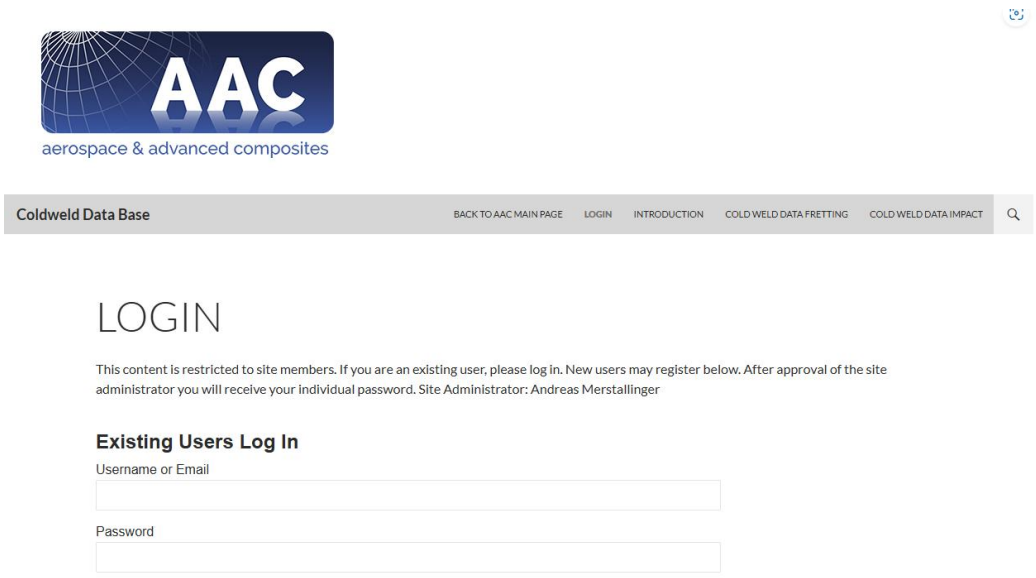

Please refer to section 9 for introduction to the data base.

5 Conclusion

1. Test equipment (Annex A) and a Test Method (Annex B) have been developed to study the cold welding of material interfaces that make contact under conditions of impact and fretting. The method and results enable to make a step forward in cold-welding effects from „common experience“ to measurable numbers, useful for designers of spacecraft applications.
2. In order to provide engineers with experimental data, a new internet data base was set up by AIT. It collects all data generated from all studies performed for ESTEC. It can be accessed free of charge after registration: http://service.arcs.ac.at/coldwelddata.
3. It was shown, that both the **theoretical predictions were by far not comparable to experimental** data. The main reason is seen, that the adhesion is driven by the “real contact area” which cannot predicted, e.g. hertzian theory would predict a “nomial contact area” neglecting surface roughness and surface contamination. Especially, the latter has the main contribution and keeps unpredictable.
4. A wide range of material pairings covering metal-metal (SS17-7 PH versus itself and Al alloy AA 7075 versus itself), metal-polymer (SS17-7 PH versus Vespel SP3), as well as several coatings for steels, aluminium and titanium were investigated under impact and fretting conditions. This data can be readily found in Annex C. These results and results of future work is searchable on the WEB.
5. Tests have revealed, that the **range of adhesion** forces in uncoated metal-metal-contact with typical engineering surfaces and without coatings **depend on the contact type**:
   - in static contact adhesion forces were below 0.5 N,
   - in impact adhesion force up to 2 N, and
   - under fretting adhesion forces in excess of 18 N were found.

   Basic material physics (type of atomic bonds) indicate that there is no technically measureable adhesion between metals and polymers and ceramics expected A few tests between steel or aluminium and polyimide did not contradict this premise.
6. In order to **avoiding cold welding** polymers or ceramics can be selected, but this may not be suitable for space hardware and their mechanisms. Hence, often metal-metal-contacts cannot be avoided. Then, the first strategy to reduce cold welding risk would be the use of **dissimilar alloy pairs**, e.g stainless steel versus hard steel (low adhesion likely). The second way is the use of coatings. However, here the type of contact and the substrate material needs to be well known.
7. Under **impact**, hard coatings on **stainless steel** (for instance TiC) may break and, therefore, adhesion is lower but still found. Soft coatings made of solid lubricants (e.g. MoS_2) can repair themselves during impact, i.e. prevention of adhesion is more efficient than for hard coatings. Stainless steels are generally too soft to support a hard coating under impact conditions. Hard anodised **aluminium** can withstand impact. **Titanium** alloy must be coated with hard coatings to resist cold welding, if only impact is expected.
8. Under **fretting** none of the investigated coatings is able to avoid cold welding of stainless steel (SS17-7PH). Also MoS_2 is not effective in fretting, lubrication is lost soon. Hence, main strategy must be the use of different steels (maximum one partner being austenitic). Hard coatings should not be on hard steels. In contrast to steel, hard anodising of **aluminium** prevents adhesion in fretting. However, much lose debris is formed. A thick “Keronite” coating (20µm), which is based on a plasma-electrolytic-oxidation process, is not only resistant to fretting but also avoids debris formation. A test campaign using uncoated **titanium** pin against coated titanium discs, did not give a “general solution”. All thin coatings -solid lubricants and hard coatings- were destroyed in the fretting contact. The best combinations still showed medium adhesion after break of the coating. Combination between titanium and low adhesion steel did also not provide a solution. Testing thick coatings produced by PEO (Keronite) Further research will target thick coatings.

6 Literature

6.1 REFERENCES

[1] *ECSS-E30 - European Co-operation for Space Standardisation (ECSS):* ECSS - E-30 "Mechanical", Part 3A "Mechanisms" , section 4.7.4.4.5 "Separable contact surfaces", page 32, Pre-Print Version June 2000.

[2] **Merstallinger A., Semerad E.**, *Tribological properties of Ga3Z1*, ESTEC Contract No 8198/89/NL/LC, WO 32, 1995.

[3] **Michael R. Johnson**, *The Galileo High Gain Antenna deployment anomaly*, California Inst. of Technology, JPL, Pasadena.

[4] **Merstallinger A., Semerad E. Dunn B.D. Störi H.,** *Study on cold welding under cyclic load and high vacuum*, 6th Europ. Space Mechanisms & Tribology Symposium, Zürich, Proceedings ESA SP-374, 1995.

[5] **Merstallinger A., Semerad E.,** *Test Method to Evaluate Cold Welding under Static and Impact Loading*, In-house-Standard by ARCS approved by ESA, Issue 2 (1998).
Uncertainty evaluation for „Test Method to Evaluate Cold Welding under Static and Impact Loading", In-home-Standard by ARC Seibersdorf research GmbH, Issue 2, audited in 2003.

[6] **Merstallinger A., Sales M., Semerad E., Dunn B.D.,** *"Reduction of cold welding by geometric parameters",* Proc. 13th European Space Mechanisms and Tribology Symposium, Vienna 2009, ESA-SP-670. (ESTEC Contract No 11760/95/NL/NB, CO65.)

[7] **Roberts E. et.al.**, *Space Tribology Handbook*, ESTL, AEA-Technology, 2001.

[8] **Merstallinger A., Semerad E., Dunn B.D.**, *Cold welding due to fretting under vacuum, Helium and air*, Proc. 7h European Space Mechanisms and Tribology Symposium, ESTEC Noordwijk (NL), Oct. 1997.

[9] **Johnson K. H.,** *Contact mechanics,* Cambridge University Press, 1985.

[10] **Persson U., Chandrasekaran H., Merstallinger A.,** *Adhesion between some tool and work materials in fretting and relation to metal cutting*, WEAR 249 (2001), p. 293-301.

[11] **Merstallinger A., Semerad E., Dunn B.D.,** *Influence of impact parameters and coatings on cold welding due to impact under high vacuum*, Proc. 8th European Space Mechanisms and Tribology Symposium, Toulouse (F), Oct. 1999. (ESTEC Contract No 11760/95/NL/NB, CO 12, 1998.)

[12] **Merstallinger A., Semerad E., Scholze P., Schmidt C.,** *Screening of contact materials for cold welding due to fretting*, ESTEC Contract No 11760/95/NL/NB, CO20, Materials Report 3150, 2001.

[13] **Shrestha S., Merstallinger A., Sickert D. and Dunn B. D.,** *Some preliminary evaluations of black coating on aluminium AA2219 alloy produced by Plasma Electrolytic Oxidation (PEO) process for space applications*, Proceedings ISMSE, ESTEC, 2003.

[14] **Merstallinger A., Semerad E., Scholze P., Schmidt C.,** *Influence of coatings on adhesion under impact*, ESTEC Contract No 11760/95/NL/NB, CO21, Materials Report 2663, 2000.

[15] **Merstallinger A., Semerad E., Costin W.,** *Influence of steel types on cold welding under fretting and impact*, ESTEC Contract No 11760/95/NL/NB, CO40.

[16] **Sales M., Merstallinger A., Costin W., Mozdzen G., Semerad E.,** *Influence of Titanium Alloy Ti6Al4V on cold welding under fretting and impact*, ESTEC contract No 11760/95/NL/NB, Co52, March 2006.

[17] **Shresta S., Dunn B.D.,** *Advanced Plasma Electrolytic Oxidation treatment for protection of light-weight materials and structures in space environment,* Surface World, Nov.2007, pp.40-44.

[18] **Merstallinger A., Semerad E., Costin W.,** *Assessment of Keronite for Cold Welding and Friction*, ESTEC Contract No 11760/95/NL/NB, CO39, Metallurgy Report No. 3522, October 2002.

[19] **Sales M., Merstallinger A., Shresta S., Dunn B.D.,** *"Combating the fretting wear and cold welding of aluminium alloys on spacecraft hardware using the plasma electrolytic oxidation (PEO) process",* SMT22 – 22nd int. Conf. on Surface Modification Technologies", Tröllhättan, Sweden, Sept.21-24, 2008. (ESTEC Contract No 11760/95/NL/NB, CO60.)

[20] **Sales M., Merstallinger A., Shresta S., Dunn B.D.,** *The fretting wear behaviour of plasma electrolytic oxide coatings on aluminium Alloys,* Proc. of the 11th ISMSE: International Symposium on Materials in Space Environment, Aix-en-Provence, September 2009. (ESTEC Contract No 11760/95/NL/NB, CO72.)

[21] **Sales M., Mozdzen G., Merstallinger A., Semerad E., Costin W.,** *COLD WELDING SUMMARY CHART Collection of data of all performed Studies*, ESTEC Contract No 11760/95/NL/NB, CO53.

6.2 MATERIAL ABBREVIATIONS AND DATA TO PUBLICATIONS

Table contains the abbreviations used above. It also gives materials' data used for calculation of test parameters.

Table 3: Materials: abbreviations and data

Abbreviation	Designation	Composition	Condition	HV daN/mm²	Yield MPa	Poisson	E GPa
Al7075	Al alloy Al AA 7075	2.1-2.9Mg1.2-1.6Cu0.18-0.28Cr5.1-6.1Zn	T7351	170	654	0.33	72
Bronze LB9	Bronze LB9 BS 1400 LB4	Cu-4-6Sn-8-10Pb-2Zn-0.25Fe-0.01Al-0.2Mn-2Ni-0.5Sb-0.1S	AR	160	130	0.34	80
SS15	Stainless Steel SS15-5 PH	14-15.5Cr3.5-5.5Ni0.15-0.45Nb<0.07C2.5-4.5Cu	H1025	393	1000	0.27	196
440C	AISI 440C	Fe-1.01C-0.47Si-0.56Mn-0.014P-<0.002S-17.81Cr-0.27Ni-0.48Mo	Harden	700	2692	0.283	200
SS17	Stainless Steel SS17-7 PH	17Cr-7Ni-1Al	PH	441	1697	0.29	210
Ti834	Ti-IMI 834	Ti5.8-Al4Sn-3.5Zn- 0.7Nb-0.5Mo-0.35Si- 0.06C	AR	334	1285	0.32	112
Ti6AV	Ti-IMI 318	Ti6Al4V	AR	338	850	0.32	105
Vespel SP3	Vespel SP3	85PI-15MoS2	AR	18	68	0.41	2.5
$AgMoS_2$	Ag/MoS2	Ag 15v% MoS2	AR	26	138	0.367	71
Ag10Cu	Ag10Cu	Ag10Cu	AR	150	620	0.367	82.7
Inconel718	Inconel718 / ASTM B 637)	Fe-53.6Ni-18.9Cr-5.3Nb-3Mo-0.98Ti-0.03C-0.13Si-0.12Mn-0.008P-0.001S-0.49Al-0.2Co-0.06Cu-0.004B	AR	348	1338	0.25	211
SS316L	AISI316L	Fe-0.011C-0.41Si-1.42Mn-0.031P-17.3Cr-11.2Ni-2.09Mo-0.05W-0.098Co-0.041V-0.026S	austenitic	175	675	0.28	190
52100	AISI52100 (SKF)	Fe-1C-0.3Si-0.4Mn-0.03P-0.03S-1.6Cr-0.3Ni-0.3Cu	AR	700	2692	0.28	200
AL 2219	AL AA 2219	6.3Cu-0.3Mn-0.18 Zr-0.1V-0.06Ti	T851	138	531	0.33	73.8

7 Annex A - Description of test devices

7.1 COLD WELDING - IMPACT AND FRETTING

This very specialised and unique equipment enables to simulate cyclic closed contact, like e.g. in relays, or at end stops, and to measure the forces necessary to re-open the contact, i.e. the adhesion forces. This effect is herein referred to as "Cold Welding", but other terms may be e.g. stiction. Two facilities cover the most dangerous types of contacts: Impact during closing and Fretting within the closed contact. The latter facility may also be adopted to fretting wear tests.
It is the aim of the test to provide designers and engineers with data on adhesion force which have to be considered in design of mechanisms, i.e. to assess on one hand cold welding on bare metal contacts and on the other hand the anti-adhesion performance of coatings. If no specific parameters are demanded, tests are done according to an in-home-specification, to enable comparison of results for different material pairings and the collection of data into a database. There was undertaken a lot of effort in the past to be able to offer Special Competence in Cold Welding Effects.

Cold welding (1) - Impact test facilities

The impact facility (Fig. A.1), one for loads up to 100 N enable the measurement of adhesion forces under vacuum between contact points after cyclic contacts, varying from static contacts (long-term compression) to slow closing cyclic contacts (static adhesion) and to impacts with impact energies up to 0.02 J.
The facilities were designed and developed in house. They consists of an UHV-system (10^{-8} mbar after bake out at 130 °C) with an ion getter pump and an air damping system for vibration free measurements. Emphasis was given to the universality of the test set up covering a wide range of impact energies, contact pressures and contact times. The contact is made between a ball and a flat disc. The ball is mounted on a pushrod, which is driven by an electromagnet. A low friction loading system enables an accuracy of 1 mN (0.1 gram) for the adhesion force measurement which is made directly above the pin in the vacuum chamber using a piezo force transducer. The transducer measures the impact force as well as the adhesion, i.e. the force needed for the separation of the two materials. Cyclic loading may be done either slowly ('static') or by an impact ('dynamic') with defined energy which is determined by the mass of the pushrod and its velocity at impact as measured by a distance sensor. The impact energy, the impact force, the contact duration, the load during contact and the separation is controlled by a computer. By variation of the ball radius - typically to 2-20 mm - the contact pressure can be adjusted to the yield strength of most materials. Optionally the contact surfaces can be cleaned in situ by glow discharge before the test. The surface roughness is characterised by profilometry.

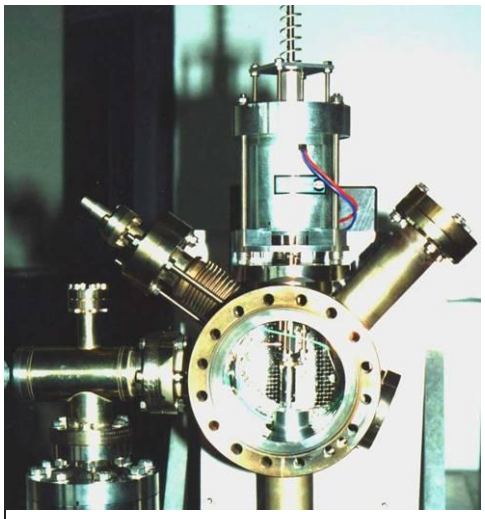

Fig. A.1 Impact facility (inside view).

Above test methods are adequate to detect the affinity of cold welding in an early state. They are capable to assess the statistical spread with increasing contact cycles in order to see if there is a tendency toward cold welding or a single catastrophic failure. A known failure of a space mechanism was successfully reproduced and studied in the laboratory. General tendencies of cold welding were assessed within a master thesis.

Cold Welding (2) - Fretting test facility

This facility (Fig. A.2) enables to investigate the influence of fretting on the tendency to the cold welding of materials, i.e. after a definite number of fretting cycles the adhesion force between contacts is measured.
The loading mechanism is analogous to the above "Cold welding - impact test device. The loading and adhesion forces are measured by the z-direction of a 3-axis piezo transducer mounted directly below the disk in vacuum. With the x-direction the friction force due to the fretting movement is measured. The fretting movement (sine, triangle or square wave) is generated by a piezo actuator for frequencies between 0 and 300 Hz and amplitudes up to 100 µm. This lateral movement is transduced to the pin via a CuBe plate and controlled at the contact by a triangulation sensor.
This facility enables for the first time the simulation of high frequency vibrations resulting e.g. from bearings combined with the measurement of adhesion force.

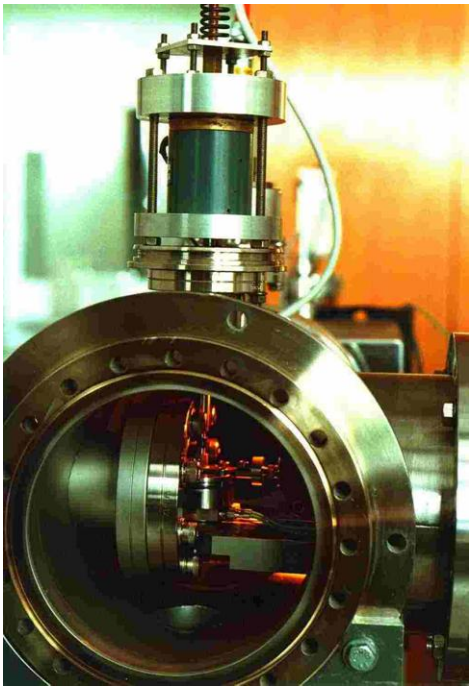

Fig. A.2 Fretting facility: device (Upside) (inside view below).

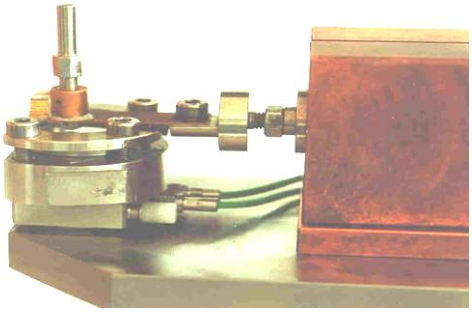

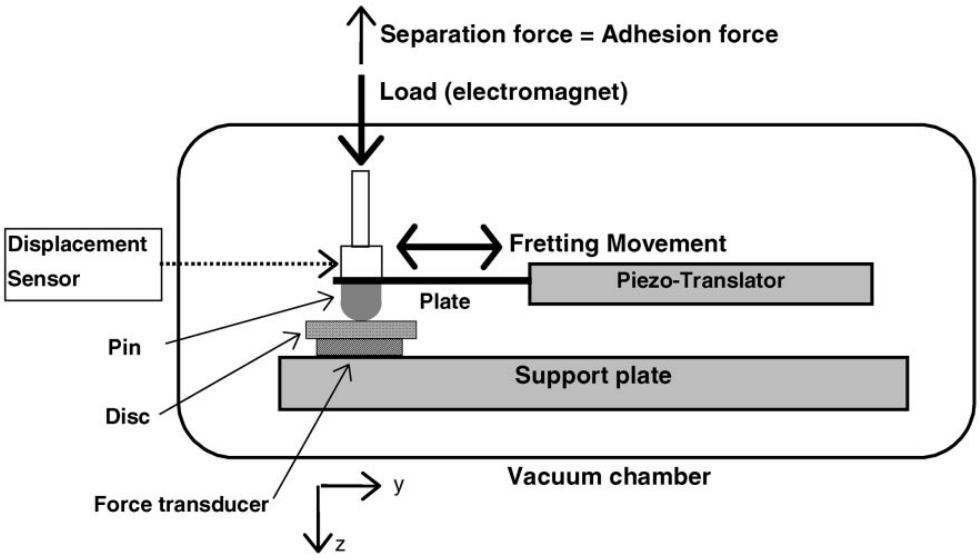

7.2 TOPOGRAPHIC ANALYSIS (PROFILOMETRY)

Topography of surfaces may be analyzed in two means: determination of “roughness” or measurement of holes or removed volume of balls after friction tests.
Surface roughness can be measured and evaluated using a PC-controlled **Stylus profilometer (RANK TAYLOR HOBSON Surtronic 3+)**. Based on international standards, calculation of all typical surface parameters any kind of profile investigation may be done by the Windows based PC-software, e.g. determination of cross sectional area of wear tracks. The maximum size of samples needed is 10 x 40 mm. this is valid for the most rough surfaces. More fine surfaces allow smaller samples. Curved specimen may also be investigated (dimensions have to be defined in detail.) Roughness can also determined inside holes or tubes (with minimum diameter of > 8mm)

8 Annex B –Test method (In-House-Standard)

Abstract

This specification describes a test determining the cold welding tendencies of materials and/ or coatings intended for use in all types of contacts that are cyclic closed and opened. Simulation of contact includes static or impact loading as well as subjecting the contact to fretting, i.e. microvibrations in direction of the contact plane. Cold welding is assessed by measuring the separation force in vertical direction, referred to as adhesion force.
This includes e.g. deployment or end-stop-mechanisms. This test is able to demonstrate the reliability of an opening device according to the cold welding section of the 'Space Mechanisms Standard Requirements Specifications'.
This specification is used to set-up a database on cold welding for common material and coating-pairings. The second issue mainly adds "fretting" as a further method. This update version 3 (2025) introduces the fretting test mode "Launch-mode": it is a short fretting test covering a sequence of 3 times 5 minutes fretting in the environments Air - Low vacuum - High vacuum. This shall simulate applications like HDRMs.

8.1 SCOPE

This specification describes a test determining the cold welding tendencies of materials and/ or coatings intended for use in all types of contacts that are cyclic closed and opened. Simulation of contact includes static or impact loading as well as subjecting the contact to fretting, i.e. microvibrations in direction of the contact plane. Cold welding is assessed by measuring the separation force in vertical direction, referred to as adhesion force.
This includes e.g. deployment or end-stop-mechanisms. This test is able to demonstrate the reliability of an opening device according to the cold welding section of the 'Space Mechanisms Standard Requirements Specifications'. This specification is used to set-up a database on cold welding for common material- and coating-pairings. Originally, all those tests were run in high vacuum. With this Issue3 also the "Launch mode" is introduced, which runs in a sequence from Air – LowVacuum - HighVacuum.

8.2 GENERAL

8.2.1 Introduction

Repeated loading and unloading of contacts results in a destruction of the surfaces' oxide layers which leads to increasing adhesion between the two parts, especially metals. Adhesion forces were found to increase in the order static contact, impact contact and fretting during static contact [B1]. Under fretting at low loads, the adhesion can even exceed the load force.
Due the fact that the opening is done by some kind of springs with limited tension, the mechanism fails, if the adhesion force exceeds the tension. This may be much less than the adhesion force which is commonly related to cold welding in sense of a real weld. The new launch mode covers the combined effect of fretting in air (additional rust creation = fretting corrosion) on the cold welding in the subsequent high vacuum phase.
This test method enables to assess the cold welding tendency of a combination of two materials with or without a coating. To avoid alignment influences, the contact is made between a pin with a spherical tip and a (flat) disc. The contact is closed and opened for several times, referred to as "cycles". During each unloading the force necessary to separate them in vertical direction, i.e. the adhesion force[1], is measured. Thereby, the maximum adhesion force is evaluated for a definite contact condition. The effect of surface cleanliness on the adhesion force may be simulated by applying a glow-discharge-(GD)-cleaning process in-situ directly before closing the contact.
The test parameters enable to set up a database which will provide designers of mechanisms with data on adhesion/cold welding.

8.2.2 Related documents

Some or all of the content of the following documents is related to this specification:

ECSS-Q-ST-20	Quality assurance requirements for ESA space systems
ECSS-Q-ST-70	Materials, mechanical parts and processes
ECSS-Q-ST-70-01	Contamination and Cleanliness control
ECSS-Q-ST70-71C	Materials, processes and their data selection
ECSS-E-ST-33-01C Rev.2	Mechanisms

ECSS "Space Mechanisms Standard Requirements Specification" (Draft):
G. Labruyère & P. Urmston, Proc. 6th European Space Mechanisms & Tribology Symposium, 1995.

The test laboratory shall also fulfil the requirements according to ISO 9001.
For comparability reasons the material and test parameters shall be documented using a standardised form[2]. (A 'Data Sheet' is provided in Annex B.)
Since this test is related to space tribology, the common requirements are based on the 'Tribometer user's guide for space mechanism applications', ESTL/TM/139, by ESTL 1995.

[1] It is presently not aim of this method to investigate "static friction force", i.e. the force needed to start sliding.

[2] DIN 50 324 'Pin-On-Disc-Wear test' was rejected on 27.11.1997. This test is also described in ASTM G99.

8.2.3 Abbreviations and Definitions

Refer to the Section 8.7.

8.3 PREPARATORY CONDITIONS

8.3.1 Hazards/safety precautions

It shall be reminded that the following devices use hazardous voltages, ion getter pumps, piezo-translators and glow-discharge-devices.

8.3.2 Materials, Specimen

8.3.2.1 Specimen

8.3.2.1.1 Identification of materials

Materials submitted for testing shall be identified by the customer according to the form given in ANNEX B. If no material data is available (Y, E, ν, H), values shall be taken from literature (E, ν), from tensile test (Y) and from hardness test (H). Calculation of yield strength from Vickers hardness test shall be avoided[3]. In case of use, Y shall be accompanied by the index 'HV': $Y_{HV} = H_V / 2.6$.

8.3.2.1.2 Dimensions

The contact geometry refers to pin (spherical shape) on disc (flat). For standard testing (except for GD), the preferred dimensions are (see Annex B for drawing):

- Pin: diameter = 6 mm, length = 8 mm (consisting of a tip of 4 mm length and an external-M3-thread with a length of 4 mm), radius of curvature is calculated by ARCS depending on the desired contact pressure, but ranges from 0.5 to 30 mm.
- Disc: diameter = 21 mm, thickness 2 - 4 mm, (for impact testing thickness up to 10 mm are possible).

If GD is applied, instead of a disc a second pin with flat surface is needed (see Annex B for drawing):

- 2 Pins: diameter = 6 mm, length = 8 mm (both including an internal-M3-thread with a length of 4mm), one with flat surface and one with curvature (radius of is calculated by ARCS depending on the desired contact pressure, but ranges from 0.5 to 30 mm).

8.3.2.1.3 Finish

The standard finish shall consist of grinding with paper to a surface roughness of:
Disc: $R_a \leq 0.1 \pm 0.02$ µm
Pin: $R_a < 0.1$ µm (curvature)

It is good practice to check the surface finish even before cleaning procedure with respect to scratches or adhering debris by visual inspection (optical microscope). Also the surface roughness has to be recorded. In case of soft materials and if no in-situ-glow-discharge is applied, this may be done after test, in order to prevent scratches resulting from the diamond stylus of the profilometer.
If not otherwise specified, the final grinding shall be done directly before the test, i.e. evacuation shall be started 30 minutes after completing the finish.
Additionally, other finishes or coatings may be chosen in order to comply with a definite application.
If the finish is not applied in-house, the samples have to be sealed into suitable bags. Then the 30 minutes to evacuation start with opening the sealing.

[3] However, this is an often used practice in tribology, since the contact refers to a similar stress situation.

8.3.2.2 Cleaning /Handling

The cleaning procedure also shall be similar to that applied during construction of the mechanism. If not otherwise specified, the following standard procedure will be done after machining and directly before test:

- ultrasonic bath in a suitable solvent for at least 10 minutes at ambient temperature
- ultrasonic bath in acetone for at least 1 minute at ambient temperature

The cleanliness has to be checked by light microscope.
These solvents are possible: ethanol (99.5%), propanol (99%), de-ionised water at 40°C (drying necessary), trichloroethan, acetone (99%). For the standard solvent a trichloroethan is used.

Handling & storage
Before and after test, until post-investigations, mechanical damage of the contacting surfaces has to be avoided. Additionally, great care has to be taken not to re-contaminate the surfaces between cleaning and test. Handling shall be done only with lintfree gloves. (For environmental conditions see below.)

8.3.2.3 Laboratory

Cleanliness
The work area shall be clean and free of dust. Air used for ventilation shall be filtered to prevent contamination of samples by moisture, oil or dust.

Environmental conditions
The room temperature shall be held constant during a test. The relative humidity shall be less than 50 % rH, the temperature shall be within 22 ± 4 °C. If a control is not possible, recording of both parameters is recommended with an accuracy of less than ± 2 °C and ± 5 % rH, respectively .

8.3.2.4 Equipment - Special apparatus

8.3.2.4.1 Description of special apparatus

The facility shall simulate the closing and opening of a mechanism. After an optional impact the contact is held closed with a defined load, within closed contact fretting may be applied but shall be stopped before unloading. At each separation the force necessary to separate pin and disc vertically, i.e. the adhesion force, shall be measured. This sequence (called cycle) shall be repeated several thousand times fully automated.

During adhesion tests the vacuum system shall be pumped by an ion getter pump to ensure vibration free measurements and avoid oil contamination (e.g. in case of diffusion pumps). Additionally, the chamber shall be fixed on a heavy ground plate which is provides vibration damping, for static testing an air damping system is required.

Before the test in-situ-glow-discharge-cleaning of the contact surfaces shall be possible. Therefore, suitable gas inlet pipes and valves, low vacuum gauges, HV-source and voltmeter are necessary. A shutter shall be available which can be moved between pin and disc during GD-process. Otherwise cross contamination occurs. Both sample surfaces have to be taken as cathodes and the vacuum chamber and the shutter shall act as anode. Additional, all parts connected to high voltage must be shielded in order to expose only the contact surfaces to the GD.

The tribo-system shall consist of a moveable pin with a spherical tip and a fixed disc. The movement of the pin shall be smooth, in order to prevent breaking of the adhesive junctions before separation. To ensure the required sensitivity, the measurement of all forces has to be done directly in the vacuum chamber. The determination of the impact energy may be done outside the vacuum chamber by measurement of the impact velocity. Loading shall be possible either slowly, i.e. static, or by an impact with defined energy.

To enable independent selection of impact energy and subsequent static load, no dead-weight-like loading systems shall be used. A preferred set-up consists of a loading mechanism using an electromagnet outside the vacuum chamber. The load is applied via a pushrod through a bellow to the pin. The pushrod itself is suspended frictionless by springs. A piezo force transducer may be used for the measurement of all forces under vacuum. At each separation the force necessary to separate pin and disc vertically, i.e. the adhesion force, must be measured.
To enable controlled impacts, a suitable electronic device is necessary to provide the electromagnet with defined energy pulses. For the determination of the impact energy the mass of the pushrod including the force sensor - the pin is neglected - and the impact velocity must be known. The latter shall be measured by an external distance sensor and shall be recorded by use of a storage oscilloscope.
If fretting is selected, it must be applied only during closed contact and stopped before unloading. A control of the horizontal force is required to reduce any lateral force, which commonly exist after stopping fretting. Otherwise junctions would be sheared off during unloading and at the separation itself no adhesion would be measured. Fretting movement may be introduced by a plate using a piezo transducer and verified by a displacement sensor. Herein, lateral and vertical forces (load, adhesion) must be measured which may be achieved by a 3-axis-force transducer below. (See Fig. 1.)
A control and data acquisition software has to be provided to fulfil the requirements given below. The main requirement is to measure and acquire adhesion force at each separation automatically.

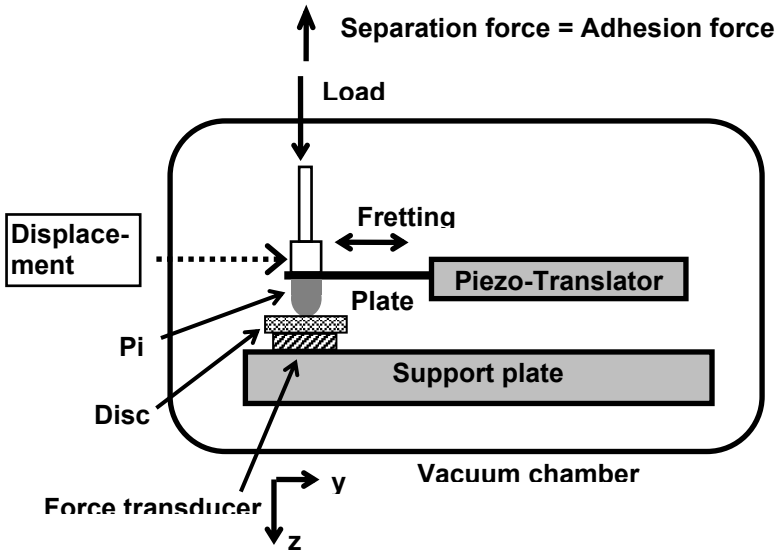

Fig. B1 Functional sketch of fretting device.

8.3.2.4.2 Technical specifications

Requirements for equipment necessary to perform tests:

Vacuum, vibration damping	ion pumps, damping system
Vacuum (base pressure)	
Static	< 1.10-8 mbar
Impact	< 5.10-8 mbar
Fretting	< 5.10-7 mbar
"Frictionless" loading system	e.g. electromagnet (PC controlled), pushrod suspended by springs
Applicable (static) loads	
Static, Impact	1 - 100 N
Fretting	1 - 40 N
Impact	
Energies	0 (static) to 0.02 J (impact)
Velocities (calculated from energies)	0 to 0.25 m/s
Contact and opening durations	selectable seconds to hours (typical: seconds)
Fretting	
Oscillating frequency	2 to 200 Hz, triangle or sin wave.
Sliding amplitude (max.)	10 - 60 µm
On/Off – Control	(Separation without fretting!)
Control of amplitude	horizontal force has to zeroed before separation

Measurement and accuracies required:

Vacuum	UHV and low vacuum gauges
Impact velocity	± 0.01 m/s, (energy: ± 2.10^{-5} J)
Static Load	± 5% of load, ± 1 N minimum
Adhesion force	
Static	± 1 mN, drift < 5 mN/min
Impact	± 10 mN
Fretting	± 50 mN
Fretting	
Sliding amplitude (max.)	± 5 µm
Horizontal force, accuracy	± 0.05 N

Fully automated control by PC is at least required for

- Cycling
- Separation sequence (adjusting of force sensitivity to highest possible value)
- Zeroing of horizontal force after fretting and before separation (a critical value is defined below)

Fully automated data acquisition by PC is at least required for

- Load
- Vacuum
- Adhesion force (value of each cycle, time resolution 25 ms)
- Backup of separation sequence for maximum adhesion

Irregularly manual data acquisition by e.g. digital storage oscilloscope is possible, if parameter is reliably constant (storage is recommended for selected post-control):

- Impact velocity,
- Impact force,
- Impact sequence (rebounds)
- Fretting frequency, amplitude

Optional equipment for surface cleaning:

Glow-discharge-cleaning	
Low Vacuum control	~ 0.2 mbar, ± 0.01 mbar,
High Voltage device	U = - 1100 ± 100 V_{DC} , I > 2 mA (recommend: 2mA/ cm^2)
HV-measurement	- 1200 ± 1 V_{DC}
Gas	Ar 5.0 with 5% H_2

Related equipment for surface and material characterisation required:

Profilometry	Mean surface roughness (R_a), max. peak-to-valley-distance (R_t)
SEM	Morphology and area of contact surfaces,
EDX	material transfer
Optical Microscope	Visual inspection (Cleanliness)
Hardness tester	recommended for rapid calculation of contact parameters
Tensile test device	(optional)

8.4 TEST PROCEDURE

8.4.1 Introduction - Selection of test method

Two criteria for selection of test parameters are possible:

1. Standard test parameters (see below).
2. Test parameters acc. to application (defined by end-user).

For the purpose of setting up a database on adhesion/cold welding data, the standard parameters should also be included, e.g. at least by parameter change during one test run. A flow chart is given in next section.

8.4.2 Test (Contact) parameters

Main objective:

To achieve comparability between tests performed on all pairings of materials with different mechanical properties, the following main parameters are chosen to be similar for all tests:

- Contact pressure relative to the elastic limit (EL),
- Impact energy (W) relative to the critical energy (W_Y).

By use of Hertz theory and the TRESCA criterion the critical static load which is related to the onset of yield, i.e. 100 % EL, can be calculated (refer to Annex A):

$$P_Y = 21.17 \frac{R^2 Y^3}{E^{*2}} \quad [N] \qquad \text{Equ. 1}$$

The critical impact energy (W_Y) which is related to the onset of plastic yield at low impact velocities may be calculated according to the dynamic Hertz theory (refer to Annex A):

$$W_Y = 53.4808 \frac{Y^5 R^3}{E^{*4}} \quad [N] \qquad \text{Equ. 2}$$

Static adhesion test:
For the contact pressure two values shall be used:

- Start test at elastic limit acc. Hertz, i.e. 100% EL
- After reaching constant adhesion level increase to 188 %EL

To achieve the required contact pressure the radius of curvature (R) can be adjusted in the range from 0.5 to approx. 30 mm. This results in static loads within the ranges 5-10 N (100 %EL) and 40-50 N (188% EL).

Impact adhesion test:
For the contact pressure three values shall be used:

- First 10.000 cycles at 40 %EL
- next 5.000 cycles at 60 %EL
- next 5.000 cycles at 100 %EL

As mentioned above, selecting a radius of curvature in the range of 0.5 to 30 enables to fulfil both static load conditions and the impact energy condition. For standard testing the impact energy shall be constant for the whole test:

- 40 * W_Y

For additional testing following impact energies are recommended:

- 200 or 4000 * W_Y

(Note: The adoption of parameters are based on studies on the influence parameters on impact performed within [B2]: higher impact energies do not increase adhesion significantly.)

Fretting adhesion test (launch mode is always done with fretting):
For the contact pressure following value shall be used:
60 %EL
This is derived from ECSS-E-ST-33-01C section 4.7.5.4.5: "… the peak hertzian contact stress shall be verified to be below 93 % of the yield limit of the weakest material." This refers to 58% of the elastic limit according to Hertz [B3].

The fretting parameters themselves refer to a frequency of 200-220 Hz and an amplitude, the "end-to-end-movement-distance", of 50 µm. Fretting shall be applied for 10 seconds and then be switched off for the separation.
Important: After fretting is stopped a lateral force remains within the contact. Before unloading this force must be decreased to a value < 0.03 N. Otherwise welded contacts would be sheared off in lateral direction during unloading, and at separation no (vertical) adhesion force would be measured.

The holding/resting durations for all test types are given in the table below. (The resting duration depends on the vacuum, i.e. the product of vacuum times resting shall be constant to achieve a defined re-coverage of surface during opening, i.e. better vacuum allows longer resting.)

Table B.1: Overview of main test parameters. (Values are theoretical calculations.)*

Contact type Parameter	Static	Impact	Fretting (Mode HV and Mode Launch)	Static with GD
Vacuum required	< 1.10^{-8} mbar	< 5.10^{-8} mbar	< 5.10^{-7} mbar	< 5.10^{-8} mbar
Impact energy	--	40 W_Y (200, 4000 W_Y)	--	--
Fretting Frequency Fretting Amplitude			200 Hz 50 µm	
Contact pressure [%EL]	100 , 188*	40, 60, 100	60	100
Static loads [N]	3 to 50	3 to 100	3 to 40	3 to 50
Holding time	30 s	10 s	10 s	1. Cycle: 900 s 30 s
Resting time	5 s	5 - 10 s	5 - 10 s	5 s

Clarification for choice of parameters
Besides that, the performed parametric investigations- done in [B2] enable to reduce testing effort: for screening only the use of one impact energy of 40 W_Y, i.e. the energy that firstly causes yield, is sufficient. (Higher impact energies did not increase adhesion significantly.) It is combined with three different static loads (40%, 60% and 100 % of elastic limit) which are applied subsequently within one test. (An increase of contact pressure can induce irreversible changes of material properties (work hardening, yield). Hence, decreasing contact load from “high to low” would probably result in a too low contact area compared to a virgin surface (e.g. contact area depends on yield strength). This could further lead to a too low adhesion value. On the other hand, for the contact properties, a previous lower load has no significant influence. Hence, testing can be done using increasing but not decreasing steps. To exclude influence of running-in effects, a duration of 10,000 cycles for the first load, and 5000 cycles for each subsequent parameter was found sufficient.

8.4.3 Test process for general spacecraft application

8.4.3.1 Flow chart

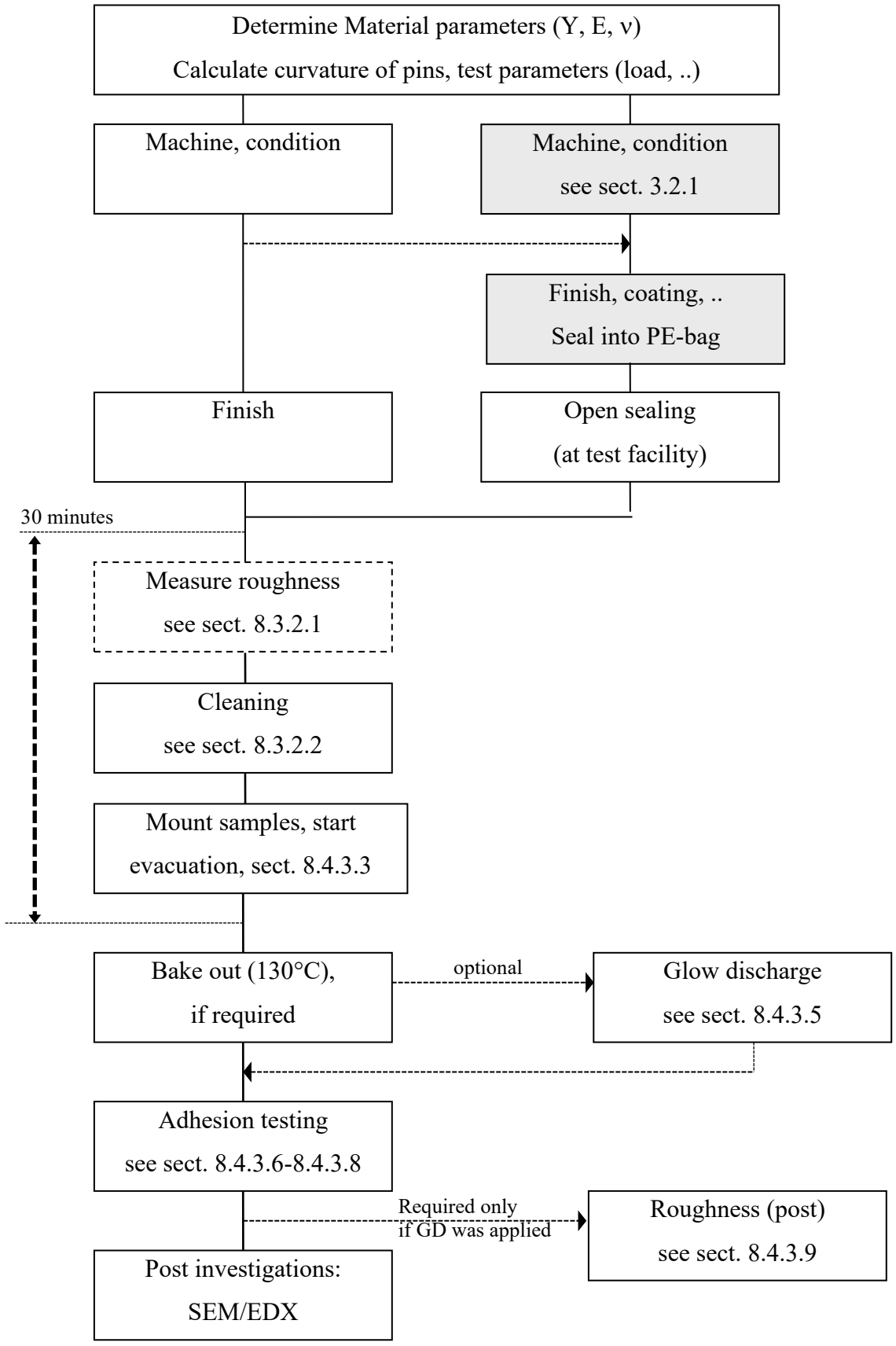

8.4.3.2 Sample preparation and pre-test-investigations

For details of sample preparation please refer to section 3.2 ‘Materials, specimen’ or to the flow chart in sect. 4.3.1.: finish, roughness, cleaning procedure, check of cleanliness, mounting of samples and start of evacuation. The duration from completion of finish, or opening the sealing, to the start of evacuation shall not exceed 30 minutes! This is only regarded as a recommendation if tests are done under fretting (either high vacuum or launch mode).

8.4.3.3 Sample mounting and functional checks

In case of impact loading the disc has to be fixed properly to avoid loosening. Care has to be taken to avoid loading the contact by the air pressure during evacuation. In case of force measurement by piezo transducers, the drift shall be low enough to ensure a correct unloading control, e.g. <5 mN/min in case of a resolution of 20mN/V. Ensure that the electrical insulation of pin and disc with respect to ground (vacuum chamber) is proper, if glow-discharge is foreseen.

8.4.3.4 Evacuation and bake out

The chamber is pumped down by a turbomolecular pump and baked out at 130 °C (50N-piezo), if it is necessary to achieve the required base pressure, i.e. for fretting testing it is not necessary. The ion getter pump may be turned on during bake out. After cooling down to room temperature, a glow discharge cleaning may be inserted to achieve clean surfaces.

8.4.3.5 Glow-discharge-cleaning-process

Before starting the DC-glow-discharge the shutter must be moved between pin and disc to avoid cross-contamination. If no surface analysis is available for determination of the cleanliness, the voltage-pressure-correlation must be observed. At constant pressure, voltage increases with reduction of impurity (oxide) layers. After voltage has become constant, the cleanliness of the surface is assumed. To improve the cleaning process, approximately 5 % H_2 shall be added to the Ar.

The parameters for the GD-cleaning process are:

gas:	Ar 5.0 with 5 % H_2,
pressure:	about 0.2 mbar, accuracy ± 0.01 mbar,
DC-voltage:	-1100 ± 50 V, accuracy ± 1 V,
current:	2 mA/cm^2,
duration:	20 min total, but at least 10 min at constant voltage, i.e $\Delta U < \pm 5V$.
resting time:	30 s between GD and first loading

Between end of glow discharge and loading of the contact a resting time of 30 seconds shall be maintained. The holding time of the first cycle shall be 15 min. Within this time the chamber is evacuated, pumping shall be overtaken by ion getter pump to ensure to continue the test vibration free. The change of the surface structure and roughness properties must be determined, if GD was applied.

8.4.3.6 Static/Impact cyclic adhesion test

In case of static loading the distance between pin and disc in the opened state shall be as low as possible to avoid vibrations induced by the movement. Check the drift of the piezo to be low.
To achieve the desired impact energy the pin-disc-distance and the impact velocity have to be adjusted. If the latter is measured, an oscilloscope may be used and the impact energy may be calculated using the mass of the pushrod:

$$W = (m\ v^2) / 2 \quad [J]$$

The parameters of the contact - load level, time of contact, time of open contact, loading/unloading speed - are controlled by the computer. It is good practice to prove the correct process control of the PC during the first ten cycles, and the acquisition of the adhesion force every few thousand cycles.

8.4.3.7 Change of parameters

For economic reasons and if only the destruction in the most severe case is of interest, the load, holding and resting duration, as well as the impact energy may be varied after a steady state was achieved by the former set of parameters. Due to the probability of work hardening the values of the load or the impact energy should only be increased. (See section 4.2 and e.g. table 1.)

8.4.3.8 End of test

In all three types of testing, the cycling may be stopped, if either

1. the steady state of the adhesion force is determinable, or
2. the standard number of cycles is fulfilled
3. the desired life-time, i.e. number of cycles, is fulfilled.

8.4.3.9 Post investigations

During unloading of the samples, the presence of debris shall be stated. Especially if GD-cleaning was applied, the change of the surface structure and the surface roughness must be determined by SEM and a profilometer, respectively. At least the contact area and a possible material transfer shall be detected. (In case of static loading and rough surfaces it may be impossible to detect the contact area, then the theoretical values may be taken.)

8.4.4 Test process for “Launch mode” related to HDRM – applications

Overall, this launch mode follows the process for fretting test (section 8.4.3). However, in the launch mode, the test is divided into 3 phases: after mounting, the test is running 5 minutes in air, is continued 5 minutes in low vacuum and then another 5 minutes in high vacuum. This shall simulate the life of HDRMs.

8.4.4.1 Flow chart fretting test in "launch mode"

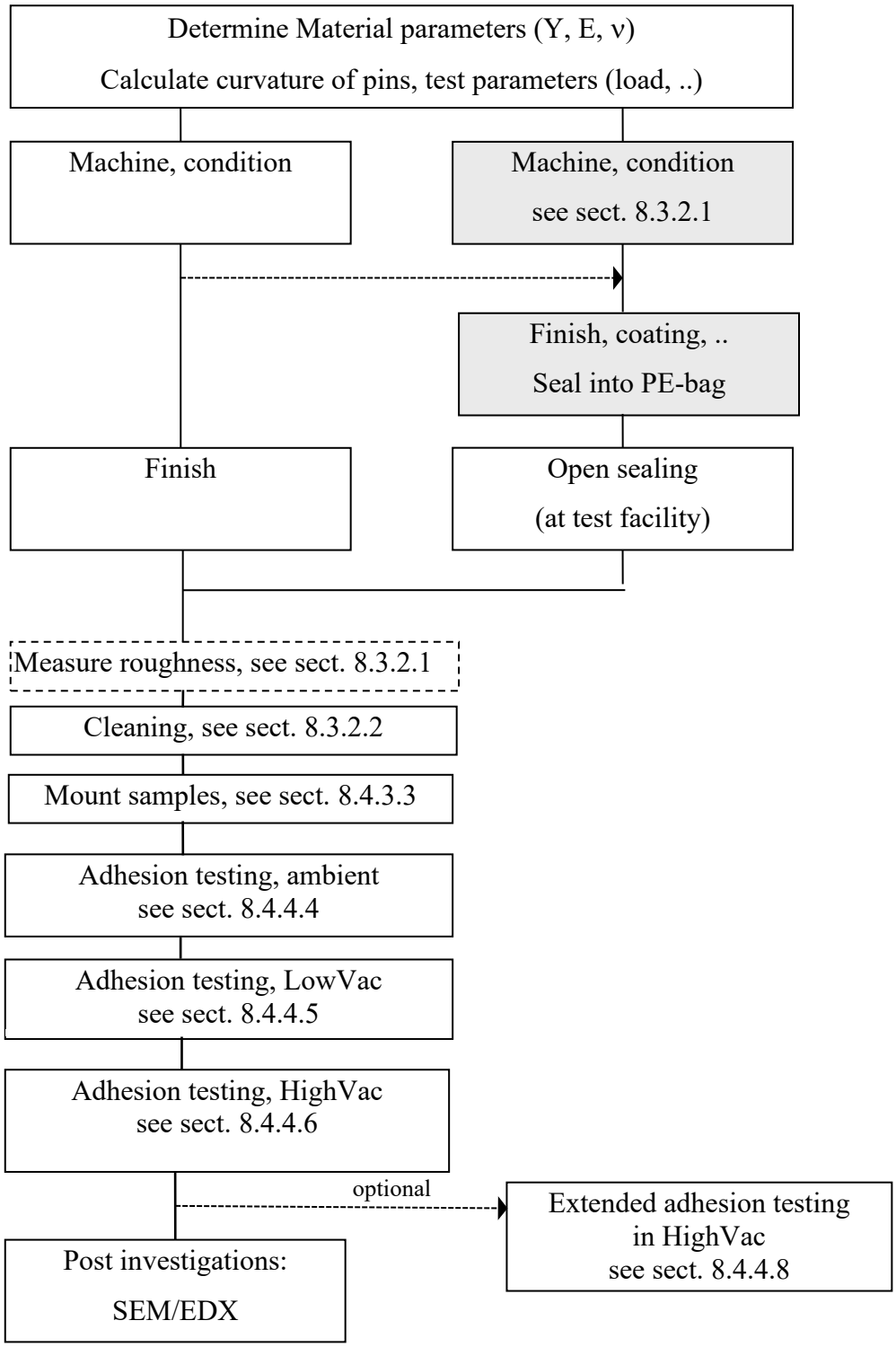

8.4.4.2 Sample preparation and pre-test-investigations
See Section 8.3.4.2

8.4.4.3 Sample mounting and functional checks
See section 8.3.4.3.

8.4.4.4 Fretting cyclic adhesion test in Ambient (Air)
At first fretting cyclic adhesion in air is done. Therefore, a humidifier shall be used to achieve 55%rH +/- 10%. The vacuum chamber is kept open. It shall be run for 30 cycles (times 10 seconds fretting reveals about 5minutest total fretting motion). After that, chamber shall be closed and low vacuum of 1-2 mbar shall be targeted. That can be achieved by use of roughing pump and a vacuum valve (LowVac). Note, that during evacuation the pin is lifted from the disc (no uncontrolled vibration in the contact).

8.4.4.5 Fretting cyclic adhesion test in LowVac (1mbar)
Keeping a vacuum level 1-2mbar, fretting cyclic adhesion is run in low vacuum for 30 cycles. After that, vacuum valve is fully opened and high vacuum pump is started. After reaching high vacuum the ion pump is started, the valve is closed and turbo and roughing pump are switched off to enable vibration free high vacuum. Note, that during evacuation the pin is lifted from the disc (no uncontrolled vibration in the contact).

8.4.4.6 Fretting cyclic adhesion test in HighVac
When vacuum level is below 5.10^{-6}mbar, fretting cyclic adhesion test can be started. 30 cycles are foreseen. After that, the launch mode is fulfilled (30+30+30 cycles = 15minutes net duration of fretting). In case that no adhesion is found so far, this test may be extended to evaluate life time in high vacuum.

8.4.4.7 Change of parameters
See section 8.4.2 and e.g. table B.1.

8.4.4.8 End of test
In launch mode, the cycling may be stopped, if either

1. High adhesion is found (range > 5000mN), or
2. the standard number of cycles is fulfilled (30+30+30), or
3. in case that an extended test or customer test is run, the desired life-time, i.e. number of cycles, is fulfilled.

8.4.4.9 Post investigations
See section 8.3.4.9.

8.5 ACCEPTANCE LIMITS

According to the ECSS-E-ST-33-01C section 4.7.5.4.5 the following mechanical requirements have to be fulfilled by the designer of space applications:

- The peak hertzian contact stress shall be verified to be below 93 % of the yield limit of the weakest material. This refers to 58% of the elastic limit according to Hertz [B3], and
- the actuator which separates the contact surfaces must provide at least 3 times the worst possible adhesion force in representative environmental condition.

⇒ Hence, if the force of the separating actuator is specified by the designer of the mechanism, the adhesion force must not exceed 30% of this force. However, the final safety factors depend from mission to mission and has to validated for each applications.

8.6 QUALITY ASSURANCE

8.6.1 Data

8.6.1.1 General

For practical reasons a test protocol including all the data mentioned below is used. With setup of the database, this protocol was replaced by a "Data-sheet", which contains the same data, but is more convenient for designers.

8.6.1.2 Material and surface data

Pin: Dimensions (radius of curvature), material (designation, composition, treatment, finish, Young's modulus, Poisson's ratio, hardness), if possible: roughness (R_a = mean roughness, R_t = maximum peak-to-valley-distance).

Disc: Dimensions (diameter, thickness), material (designation, composition, treatment, finish, Young's modulus, Poisson's ratio, hardness), roughness (R_a, R_t).

8.6.1.3 Test Parameters

Medium/Environment: air, gas-type, pressure,

Cleaning: before: US, in-situ-glow-discharge-cleaning,

Tribological parameters: geometry, impact (actual energy and critical value to initiate yield, peak force), static load(s) and corresponding Hertz pressures, holding and resting time(s), cycles when parameters were changed (e.g. load, pressure, end of test), temperature, fretting frequency and amplitude.

8.6.1.4 Results

Adhesion force: at beginning, maximum for each set of parameters, total maximum value,

Common description: diameter of contact area (if detectable), change of surface structures and material transfers of pin and disc, presence of debris.

Additional:

Diagram: Adhesion force, mean and maximum of an interval of 100 cycles, as function of cycles.

8.6.2 Nonconformance

Any nonconformance has to be dispositioned, e.g. interrupt due to power failure.

8.6.3 Calibration

Each measuring equipment including the data acquisition shall be calibrated. Any suspected or actual failures will be documented.

8.6.4 Traceability

To ensure traceability each specimen is accompanied by a sample-life-sheet. All tests themselves are secondly documented.

8.7 ABBREVIATIONS AND DEFINITIONS

8.7.1 Abbreviations – Properties

US ..... ultrasonic (bath)
GD ..... glow discharge
HV ..... High voltage
SEM ..... scanning electron microscope
rH..... relative humidity

R_a ..... mean roughness (arithmetic),
R_t ..... maximum peak-to-valley-distance

Contact parameters:
H_V ..... Vickers hardness
Y ..... Yield strength
Y_{HV} ..... Yield strength calculated from Vickers hardness
p_m ..... mean contact pressure in contact area
p_0..... maximum contact pressure
P..... load (P_Y refers to load at elastic limit)
R ..... radius of curvature (Spherical to flat contact, otherwise refer to e.g. [B3])
E..... Young's modulus (of material 1: E_1)
ν..... Poisson's ratio (of material 1: ν_1)
E* ..... reduced Young's modulus (Formula see next section)
W ..... impact energy (W_Y refers to W which firstly causes yield)
m..... mass (herein of pushrod)
v ..... velocity

8.7.2 Hertz Theory of elastic contact

The following formulas are used to calculate the diameter of contact (a), the maximum contact pressure (p_0) and the mean contact pressure acting in a spherical-shaped contact within the elastic regime (for theory refer to e.g. [B3] page 93f):

$$\frac{1}{E^*} = \frac{1-\nu_1^{\,2}}{E_1} + \frac{1-\nu_2^{\,2}}{E_2} \qquad [\text{Pa}]^{-1} \qquad \text{Equ. B1}$$

$$a = \left(\frac{3PR}{4E^*}\right)^{1/3} \qquad [\text{m}] \qquad \text{Equ. B2}$$

$$p_0 = \frac{3}{2}p_m = \frac{3P}{2\pi a^2} = \left(\frac{6PE^{*2}}{\pi^3 R^2}\right)^{1/3} \qquad [\text{Pa}] \qquad \text{Equ. B3}$$

The elastic limit is related to the onset of yield (which occurs not at the surface but inside the softer material). Both criteria, Tresca and von Mises yield the same relation: (see [B3] page 155):

$$p_0 = 1.60Y \qquad [\text{Pa}] \qquad \text{Equ. B4}$$

$$P_Y = \frac{\pi^3 R^2}{6E^{*2}}\left(p_0\right)_Y^3 \qquad [\text{N}] \qquad \text{Equ. B5}$$

Thus the load (P_Y) necessary to cause onset of yield follows:

$$P_Y = \frac{\pi^3 R^2}{6E^{*2}}\left(1.60Y\right)^3 = 21.17\frac{R^2Y^3}{E^{*2}} \qquad [\text{N}] \qquad \text{Equ. B6}$$

Using the yield criterion, Hertz theory also offers to calculate the (kinetic) energy (WY) necessary to cause yielding (see [B3], page 361):

$$W_Y = 53.4808\frac{Y^5R^3}{E^{*4}} \qquad [\text{J}] \qquad \text{Equ. B7}$$

For definition of the impact velocity at ARCS the mass of 0.48 kg is used:

$$v = \sqrt{\frac{2W}{m}} = 2.041\sqrt{W} \qquad [\text{m/s}] \qquad \text{Equ. B8}$$

8.7.3 Definitions – Adhesion Properties

Adhesion force:	force needed to separate two bodies in vertical direction.
Adhesion coefficient:	adhesion force divided by the (static) load (i.e. the load applied after impact, not the impact-force.)
Static friction force:	force needed to start sliding, i.e. to shear off junctions in contact plane, also referred to as stiction, sticking..

8.7.4 Definitions – Quality assurance

Nonconformance:
An apparent or proven condition of any item or documentation that does not conform to the specified requirements or which could lead to incorrect operation or performance of the item or mission. The term nonconformance is also used for failure, discrepancy, defect, anomaly, malfunction, deficiency, etc.

Traceability:
The ability to trace the history, application, use and location of an item through the use of recorded identification numbers.

8.7.5 References to Annex B

[B1] A. Merstallinger, E. Semerad, E. Preissner, P. Scholze,
"Influence of Fretting on Cold Welding of Stainless Steel SS440C versus Ti-IMI 834 under Vacuum, Helium and Air", ESTEC Contract No 9198/89/NL/LC, Work Order No. 46, March 1997.

[B2] A. Merstallinger, E. Semerad, P. Scholze,
" Influence of impact parameters on adhesion - Repeatability of Test Results",
ESTEC Contract 11760/95/NL/NB, Call-off Order No 12, June 1998.

[B3] K. H. Johnson, 'Contact mechanics', Cambridge University Press, 1985.

8.8 DIMENSIONS, FORMS

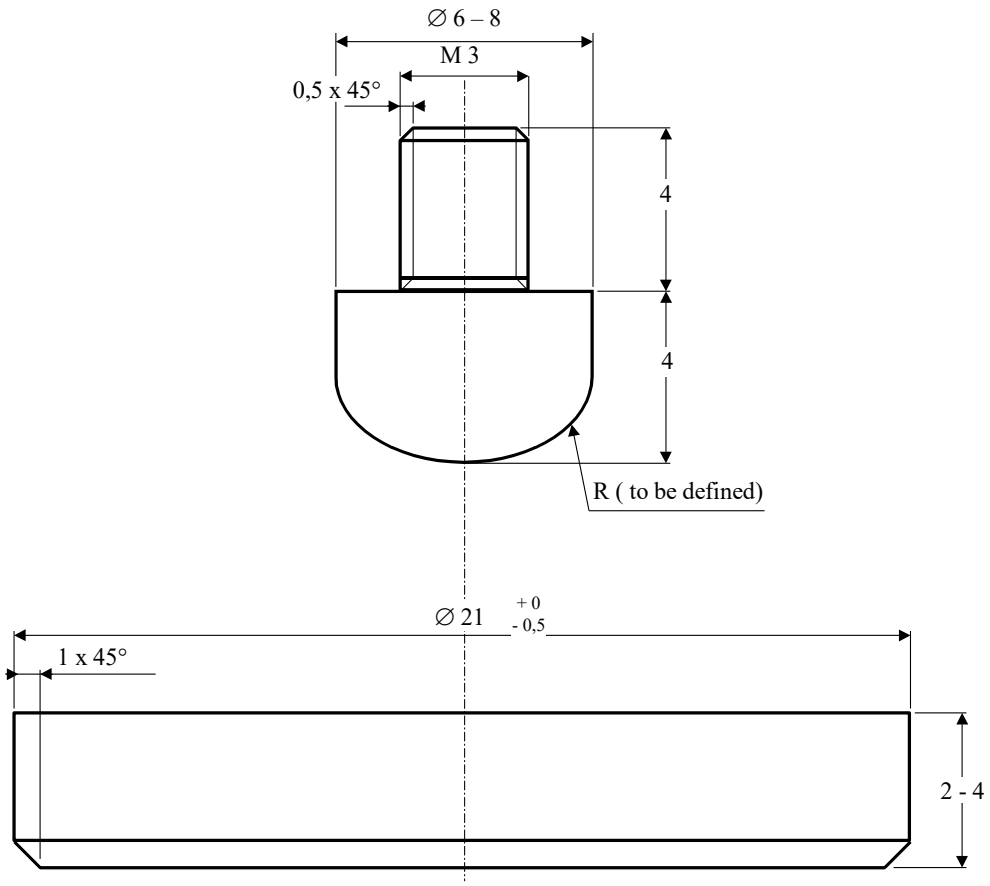

Specimen for Static, Impact, Fretting Tests

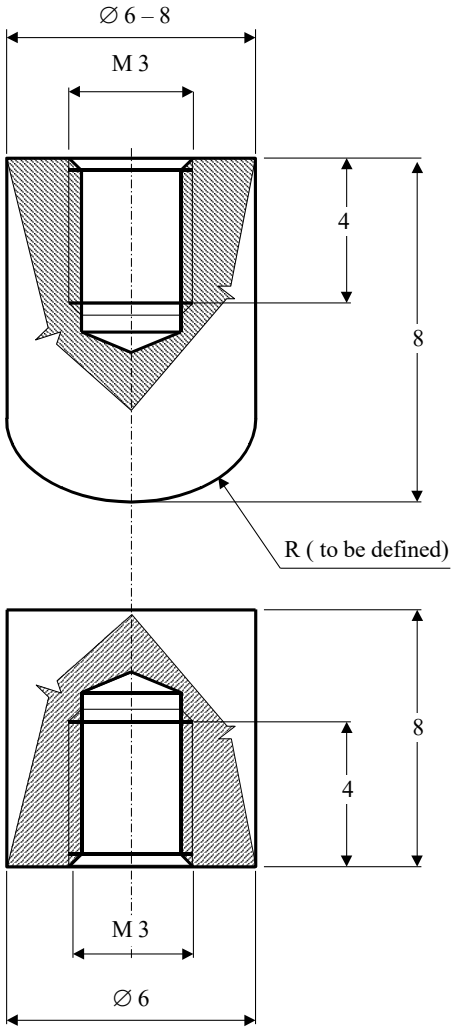

Specimens for GD-Test

9 Annex C – "Cold weld data" base (Summary charts)

In the following the Summary chart are printed. They were printed by date of July 2009 (Issue date of this document). Actual data can be obtained from the WEB:
https://coldweld.aac-research.at/

They are based on the classification as discussed above. (See image below). In the WEB-version click on the symbol opens the data sheet for the test (with all details on materials, test parameters and results).

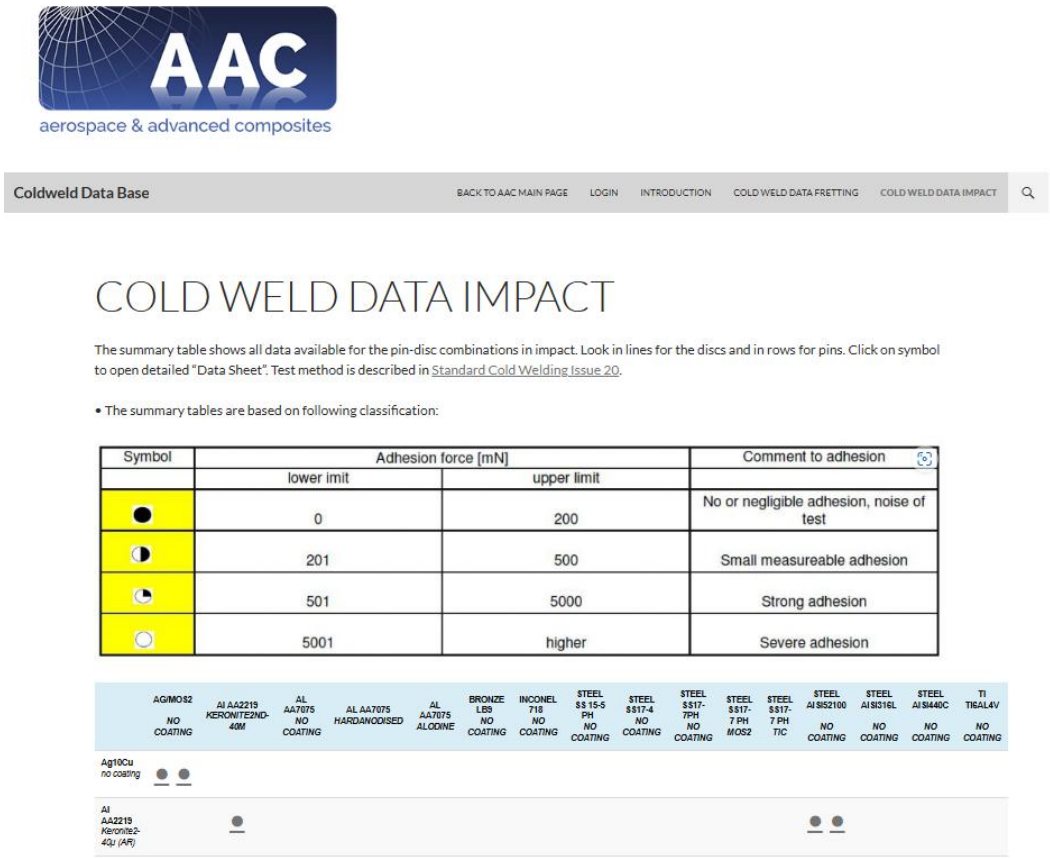

aerospace & advanced composites

Coldweld Data Base | BACK TO AAC MAIN PAGE | LOGIN | INTRODUCTION | COLD WELD DATA FRETTING | COLD WELD DATA IMPACT

COLD WELD DATA FRETTING

The summary table shows all data available for the pin-disc combinations in fretting. Look in lines for the discs and in rows for pins. Click on symbol to open detailed "Data Sheet". Test method is described in Standard Cold Welding Issue 20.

• The summary tables are based on following classification:

Symbol		Adhesion force in mN		Comment to adhesion
vacuum only	launch conditions	lower limit	upper limit	
●	●	0	200	No or negligible adhesion, noise of test
◑	◑	201	500	Small measurable adhesion
◔	◔	501	5000	Strong adhesion
○	○	5001	higher	Severe adhesion

	AG/MO 92 NO COATING	AL AA2219 KERONITE 2ND 40M	AL AA7075 NO COATING	AL AA7075 HARD ANODIZED	COPPER (CU) NO COATING	BRONZE LBS NO COATING	INCONEL 718 NO COATING	INVAR M93 FE35-36,5NI0,2-0,4MN	MOLYBDENUM (MO) NO COATING	MU-METAL (PERMALLOY) NO COATING	SILVER (AG) NO COATING	STEEL SS 15-5 PH NO COATING	STEEL SS 17-4 NO COATING	STEEL SS17-7 PH NO COATING	STEEL SS17-7 PH TIC	STEEL AI SI 52100 NO COATING	STEEL AI SI 316L NO COATING	STEEL AI SI 440C NO COATING	TI 6AL4V NO COATING	TI IMI 318 NO COATING	TUNGSTEN (W) NO COATING
Ag10Cu no coating	◔																				
Al AA2219 Keronite 2-40µ (AR)		◑														● ●					
Al AA2219 Keronite2-40µ (TC)																● ●					
Al AA2219 Keronite3-17µ (AR/TC)																● ●					
Al AA2219 Keronite3-22µ+MoS2 (AR/TC)																● ●					
Al AA2219 Keronite3-35µ (AR/TC)																● ●					
Al AA2219 Keronite3-55µ +MoS2 (AR/TC)																● ●					
Al AA6082 Keronite3-30µ (AR/TC)																● ●					
Al AA7075 no coating			○																		
Al AA7075 NiCr-plated				●																	
Al AA7075 Hard Anodised												◑									
Al AA7075 Alodine			◔																		
Al AA7075 Keronite3-40µ (AR/TC)																● ● ●					
Al AA7075 Keronite3-55µ MoS2 (AR/TC)																● ●					